Copy
RM L53F29

NACA RM L53F29

NACA

RESEARCH MEMORANDUM

TRANSONIC FLIGHT MEASUREMENT OF THE AERODYNAMIC LOAD ON THE EXTENDED SLAT OF THE DOUGLAS D-558-II RESEARCH AIRPLANE

By James R. Peele

Langley Aeronautical Laboratory
Langley Field, Va.

NATIONAL ADVISORY COMMITTEE
FOR AERONAUTICS

WASHINGTON
August 27, 1953

[redacted]

NATIONAL ADVISORY COMMITTEE FOR AERONAUTICS

RESEARCH MEMORANDUM

TRANSONIC FLIGHT MEASUREMENT OF THE AERODYNAMIC LOAD ON THE EXTENDED SLAT OF THE DOUGLAS D-558-II RESEARCH AIRPLANE

By James R. Peele

SUMMARY

A flight investigation of the aerodynamic loads on a partial-span extended leading-edge slat on the 35° sweptback wing of the Douglas D-558-II research airplane has been made. The loads data were obtained from strain-gage measurements through the airplane normal-force-coefficient range at several Mach numbers from 0.45 to 0.98.

Little change in slat normal-force coefficient at a given airplane normal-force coefficient was noted up to a Mach number of 0.65. Above a Mach number of 0.65 there was a gradual decrease of slat normal-force coefficient with increase in Mach number to 0.98 at the lower airplane normal-force coefficients. The decrease of slat normal-force coefficient with increase in Mach number was more abrupt at the higher airplane normal-force coefficients.

INTRODUCTION

The problem of the decrease in longitudinal stability during maneuvering flight introduced by the use of sweptback wings on aircraft is being investigated by the National Advisory Committee for Aeronautics as part of the joint Air Force-Navy-NACA transonic flight research program (ref. 1). As a possible solution of the stability problem of swept-wing airplanes it has been suggested that the use of leading-edge slats, mainly used for the improvement of lateral control near the stall, might be beneficial in maneuvering flight at high speeds. Information on loads that might be encountered in flight at high speeds on leading-edge slats of swept-wing airplanes is very limited (see refs. 2 and 3).

[redacted]

In order to obtain slat-loads data at high subsonic speeds, an investigation with the slats locked open has been conducted by the NACA High-Speed Flight Research Station using the air-launch version of the Douglas D-558-II (rocket and turbojet) research airplane. During this investigation flight data were obtained from accelerated maneuvers to high normal-force-coefficient values through the Mach number range to a Mach number of approximately 0.98. This paper presents the slat loads encountered during this investigation.

SYMBOLS

$b/2$	wing semispan (150 in.)
C_{N_A}	airplane normal-force coefficient, Wn/qS
C_{N_S}	slat normal-force coefficient, L_S/qS'
c_s	slat chord (9.14 in.)
g	acceleration due to gravity, ft/sec^2
h_p	pressure altitude, ft
L_S	right-slat load, lb
M	free-stream Mach number
n	airplane normal acceleration, g units
q	free-stream dynamic pressure, lb/sq ft
R	Reynolds number, based on airplane mean aerodynamic chord
S	wing area, including area projected through fuselage (175 sq ft)
S'	right-slat area (6.8 sq ft)
W	airplane gross weight, lb

[redacted]

AIRPLANE AND TEST SLAT

A photograph and a three-view drawing of the Douglas D-558-II research airplane are presented in figures 1 and 2, respectively. Physical characteristics of the airplane are listed in table I. The wing has inboard fences located 54 inches from airplane center line, and constant-chord slats. The slats may be locked in a closed position, unlocked and allowed to assume a position which is a function of the angle of attack, or locked in the open position. The data presented in this paper are for the slats locked in the open position.

A photograph of the wing with the slat in the locked-open position is shown in figure 3. A plan form and cross-sectional view of the position of the slat referenced to the wing in the locked-open configuration is presented in figure 4. The slat normal-force coefficient used in this paper is taken perpendicular to the slat chord shown in figure 4.

INSTRUMENTATION

Standard NACA instrumentation was installed in the airplane to measure the following quantities pertinent to this investigation:

Airspeed
Altitude
Normal acceleration at center of gravity of airplane
Airplane angle of attack and sideslip

METHODS

An NACA high-speed pitot-static head was mounted on a boom 0.95 maximum fuselage diameter forward of the nose of the airplane. The angle-of-attack and angle-of-sideslip vanes were mounted on the boom about 3.5 feet forward of the airplane nose. The airspeed position error introduced by the pressure field in the vicinity of the head was calibrated from $M = 0.55$ to $M = 0.80$ by the "fly-by" method and above $M = 0.80$ by the NACA radar phototheodolite method.

A strain-gage bridge was installed on each of the four rails which connect the slat to the wing. (See fig. 3 for rail locations.) These gages were calibrated in terms of known static loads which were applied normal to the slat chord at many points on the slat. This static calibration was used to evaluate the measured flight loads on the right slat.

[redacted]

The measured flight loads obtained are a combination of aerodynamic and inertia loads. The loads presented in this paper have been corrected for the effects of inertia and represent aerodynamic loads.

TESTS

The aerodynamic loads encountered on the right slat in accelerated flight were measured during wind-up turns. The flight envelopes investigated for the airplane are presented in figure 5 where the Reynolds number, based on wing mean aerodynamic chord, and airplane normal-force coefficient are plotted against Mach number. The boundary showing the start of decay of longitudinal stability taken from reference 1 has been placed in the airplane normal-force-coefficient - Mach number envelope (fig. 5) and shows the extent of coverage of these tests into the instability area with the airplane in the original configuration, inboard fences and slats closed.

The tests were made at altitudes of around 19,000 to 36,000 feet at free-stream dynamic pressures of 140 to 375 pounds per square foot.

PRESENTATION OF DATA

The aerodynamic loads measured on the right slat during flight are presented as slat normal-force coefficients. The variations of slat normal-force coefficient with airplane normal-force coefficient and airplane angle of attack at different Mach numbers are presented in figures 6 and 7, respectively. Included in each figure is the Mach number variation and pressure altitude during the maneuver. To show better the slat normal-force-coefficient variation with Mach number, figure 8 presents a summary plot of the C_{N_S} variation with M at constant values of C_{N_A}.

RESULTS AND DISCUSSION

The slat normal-force coefficients obtained from strain-gage measurements of the right-slat loads show the slope of the slat normal-force-coefficient variation with airplane normal-force coefficient dC_{N_S}/dC_{N_A} to be increasing with increase in airplane normal-force coefficient throughout the Mach number range of $M \approx 0.45$ to $M \approx 0.98$ (fig. 6). From an inspection of figures 7(a), (b), (c), (d), (e), and

(i) there are indications that the C_{N_S} values of approximately 2.2 to 2.4 obtained are peak slat normal-force coefficients for Mach numbers of 0.44, 0.45, 0.52, 0.57, 0.59, and 0.80. These peak C_{N_S} values occur at C_{N_A} values (figs. 6(a), (b), (c), (d), (e), and (i)) of approximately 100 percent of the peak C_{N_A} at $M \approx 0.45$ and decrease to about 95 percent at $M \approx 0.80$. Above the peak C_{N_S} values of approximately 2.2 to 2.3 at Mach numbers of 0.44, 0.52, 0.57, 0.59, and 0.80 (figs. 6(a), (c), (d), (e), and (i)) there is a decrease in C_{N_S} with a further increase in C_{N_A}; however, at $M = 0.45$ (fig. 6(b)) a C_{N_S} value of 2.38 at $C_{N_A} = 1.22$ was obtained without any indication of a decrease in C_{N_S} with further increase in C_{N_A}.

Below an airplane normal-force coefficient of 0.9 little change in slat normal-force coefficient at a given airplane normal-force coefficient is experienced up to $M \approx 0.65$; however, as shown in figure 8, for a value of $C_{N_A} = 1.0$ there is an increase in C_{N_S} to $M \approx 0.65$. Increasing the Mach number above $M \approx 0.65$ brings about a reduction of slat normal-force coefficient. This reduction of slat normal-force coefficient continued to $M \approx 0.98$, the highest Mach number obtained, and is of a gradual nature at the lower airplane normal-force coefficients, but increases in abruptness at the higher airplane normal-force coefficients.

CONCLUSIONS

Results of a flight investigation of aerodynamic loads over an extended leading-edge slat on the 35° sweptback wing of the Douglas D-558-II research airplane indicate the following conclusions:

1. Throughout the Mach number range tested, from approximately 0.45 to approximately 0.98, the slat normal-force coefficient increased with an increase in airplane normal-force coefficient until peak slat normal-force-coefficient values of approximately 2.2 to 2.4 at Mach numbers of 0.44, 0.45, 0.52, 0.57, 0.59, and 0.80 were obtained. Above the peak slat normal-force-coefficient values there was a decrease of slat normal-force coefficient with a further increase of airplane normal-force coefficient except at a Mach number of 0.45.

2. Below a Mach number of approximately 0.65 there is little change in slat normal-force coefficient with increase in Mach number at a given airplane normal-force coefficient except at an airplane normal-force coefficient of 1.0 where there is a gradual increase of slat normal-force

coefficient with increase of Mach number. Between a Mach number of approximately 0.65 to 0.98 there is a reduction of slat normal-force coefficient with increase in Mach number at all values of airplane normal-force coefficient tested.

Langley Aeronautical Laboratory,
National Advisory Committee for Aeronautics,
Langley Field, Va., June 9, 1953.

REFERENCES

1. Fischel, Jack, and Nugent, Jack: Flight Determination of the Longitudinal Stability in Accelerated Maneuvers at Transonic Speeds for the Douglas D-558-II Research Airplane Including the Effects of an Outboard Wing Fence. NACA RM L53A16, 1953.

2. Cahill, Jones F., and Nuber, Robert J.: Aerodynamic Load Measurements Over a Leading-Edge Slat on a 40° Sweptback Wing at Mach Numbers From 0.10 to 0.91. NACA RM L52G18a, 1952.

3. Kelly, John A., and Hayter, Nora-Lee F.: Aerodynamic Characteristics of a Leading-Edge Slat on a 35° Swept-Back Wing for Mach Numbers From 0.30 to 0.88. NACA RM A51H23, 1951.

[redacted]

TABLE I.- PHYSICAL CHARACTERISTICS OF THE DOUGLAS

D-558-II AIRPLANE

Wing:	
Root airfoil section (normal to 0.30 chord)	NACA 63-010
Tip airfoil section (normal to 0.30 chord)	NACA 63_1-012
Total area, sq ft	175.0
Span, ft	25.0
Mean aerodynamic chord, in.	87.301
Root chord (parallel to plane of symmetry), in.	108.51
Tip chord (parallel to plane of symmetry), in.	61.18
Taper ratio	0.565
Aspect ratio	3.570
Sweep at 0.30 chord, deg	35.0
Incidence at fuselage center line, deg	3.0
Dihedral, deg	-3.0
Geometric twist, deg	0
Total aileron area (aft of hinge), sq ft	9.8
Aileron travel (each), deg	$\pm$15
Total flap area, sq ft	12.58
Flap travel, deg	50
Horizontal tail:	
Root airfoil section (normal to 0.30 chord)	NACA 63-010
Tip airfoil section (normal to 0.30 chord)	NACA 63-010
Area (including fuselage), sq ft	39.9
Span, in.	143.6
Mean aerodynamic chord, in.	41.75
Root chord (parallel to plane of symmetry), in.	53.6
Tip chord (parallel to plane of symmetry), in.	26.8
Taper ratio	0.50
Aspect ratio	3.59
Sweep at 0.30 chord line, deg	40.0
Dihedral, deg	0
Elevator area, sq ft	9.4
Elevator travel, deg	
Up	25
Down	15
Stabilizer travel, deg	
Leading edge up	4
Leading edge down	5

[redacted]

TABLE I.- PHYSICAL CHARACTERISTICS OF THE DOUGLAS

D-558-II AIRPLANE - Concluded

Vertical tail:	
Airfoil section (parallel to fuselage center line)	NACA 63-010
Area, sq ft	36.6
Height from fuselage center line, in.	98.0
Root chord (parallel to fuselage center line), in.	146.0
Tip chord (parallel to fuselage center line), in.	44.0
Sweep angle at 0.30 chord, deg	49.0
Rudder area (aft the hinge line), sq ft	6.15
Rudder travel, deg	±25
Fuselage:	
Length, ft	42.0
Maximum diameter, in.	60.0
Fineness ratio	8.40
Speed-retarder area, sq ft	5.25
Power plant:	
Turbojet	J-34-WE-40
Rocket	LR8-RM-6
Airplane weight (full jet and rocket fuel), lb	15,131
Airplane weight (full jet fuel), lb	11,942
Airplane weight (no fuel), lb	10,382
Center-of-gravity locations:	
Full jet and rocket fuel (gear up), percent mean aerodynamic chord	23.5
Full jet fuel (gear up), percent mean aerodynamic chord	25.2
No fuel (gear up), percent mean aerodynamic chord	27.0
No fuel (gear down), percent mean aerodynamic chord	26.4

NACA

[redacted]

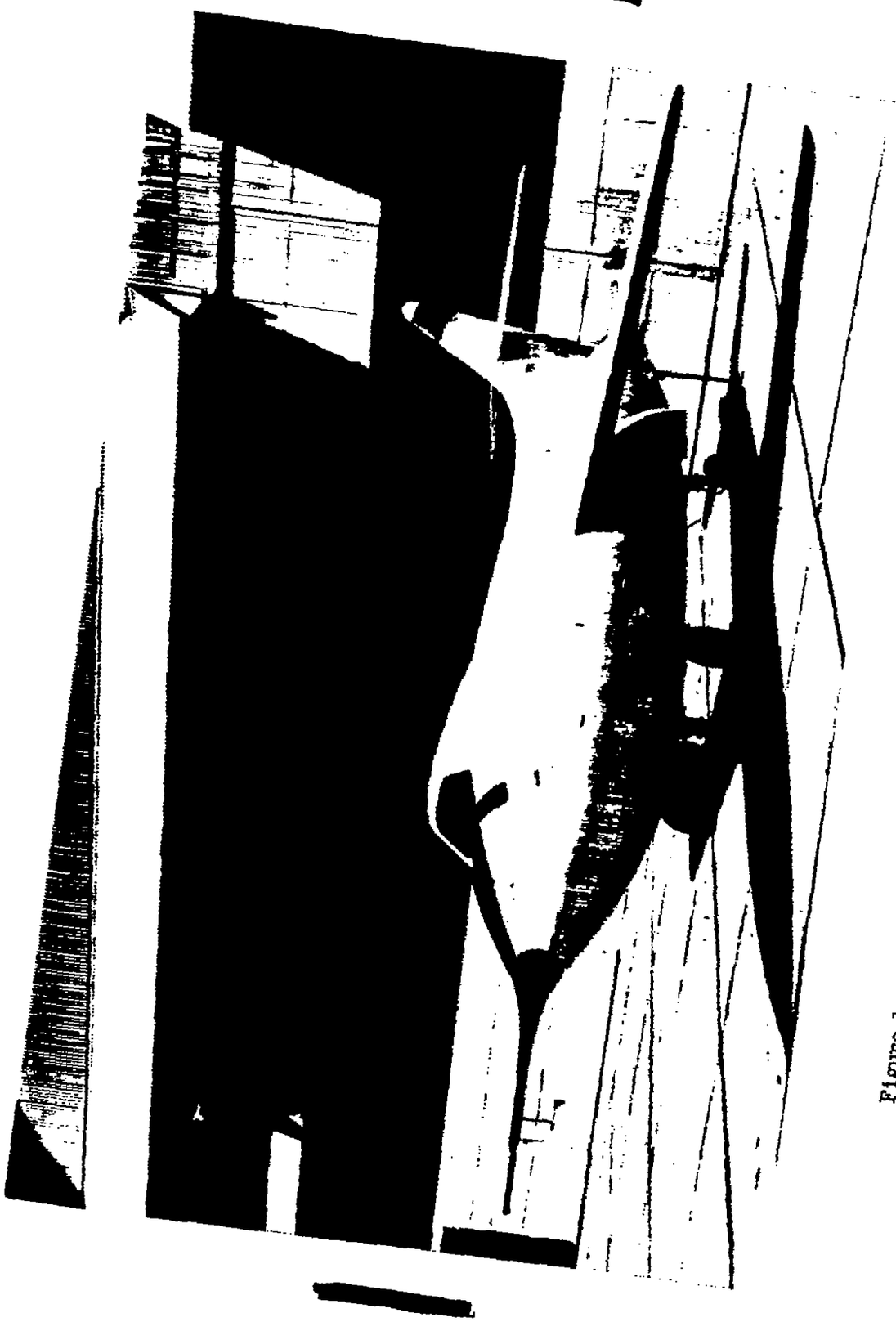

Figure 1.- Three-quarter front view of Douglas D-558-II airplane.

LE-488

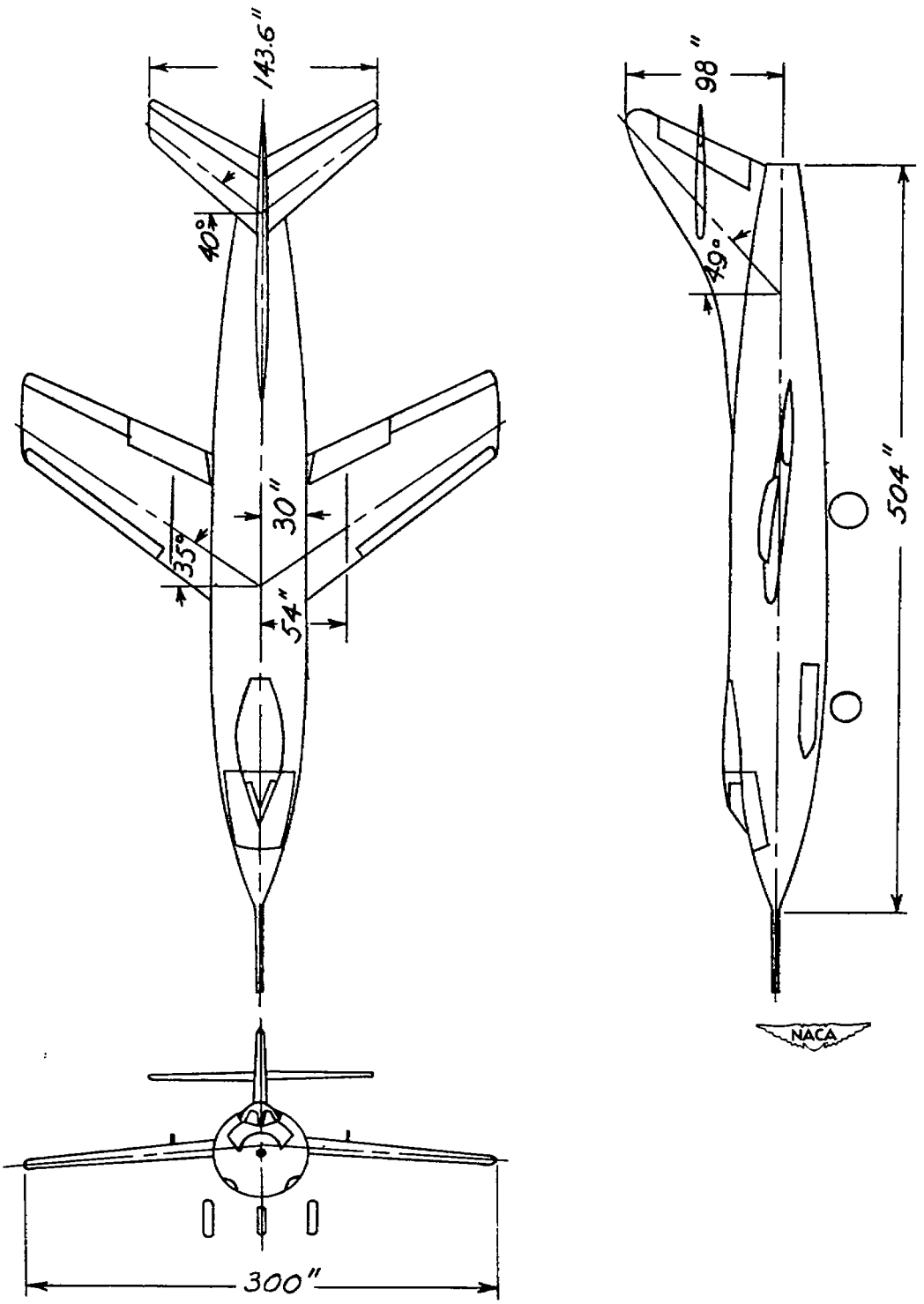

Figure 2.- Three-view drawing of D-558-II airplane.

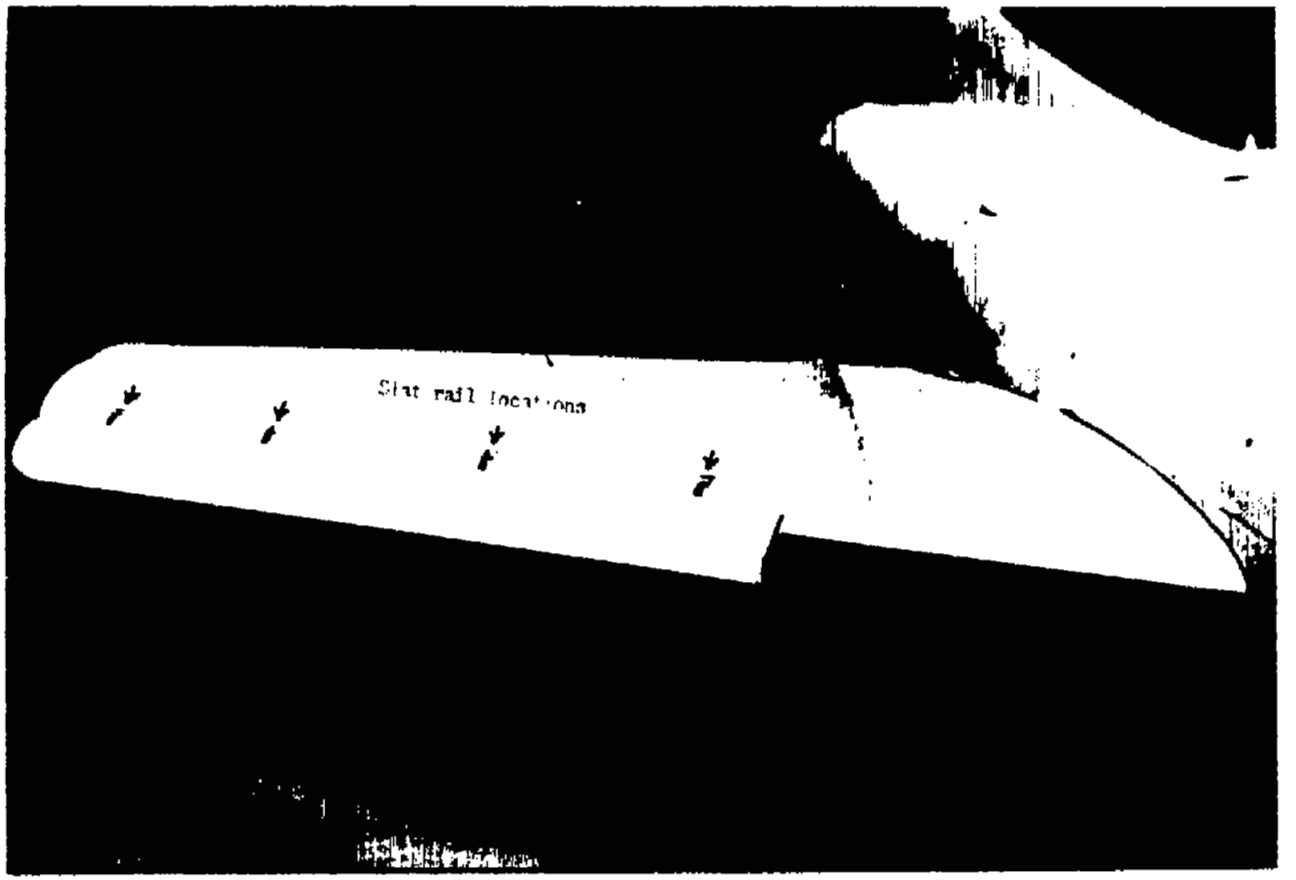

LE-817.1

Figure 3.- Photograph of the wing of the D-558-II airplane showing the slat in the locked-open position.

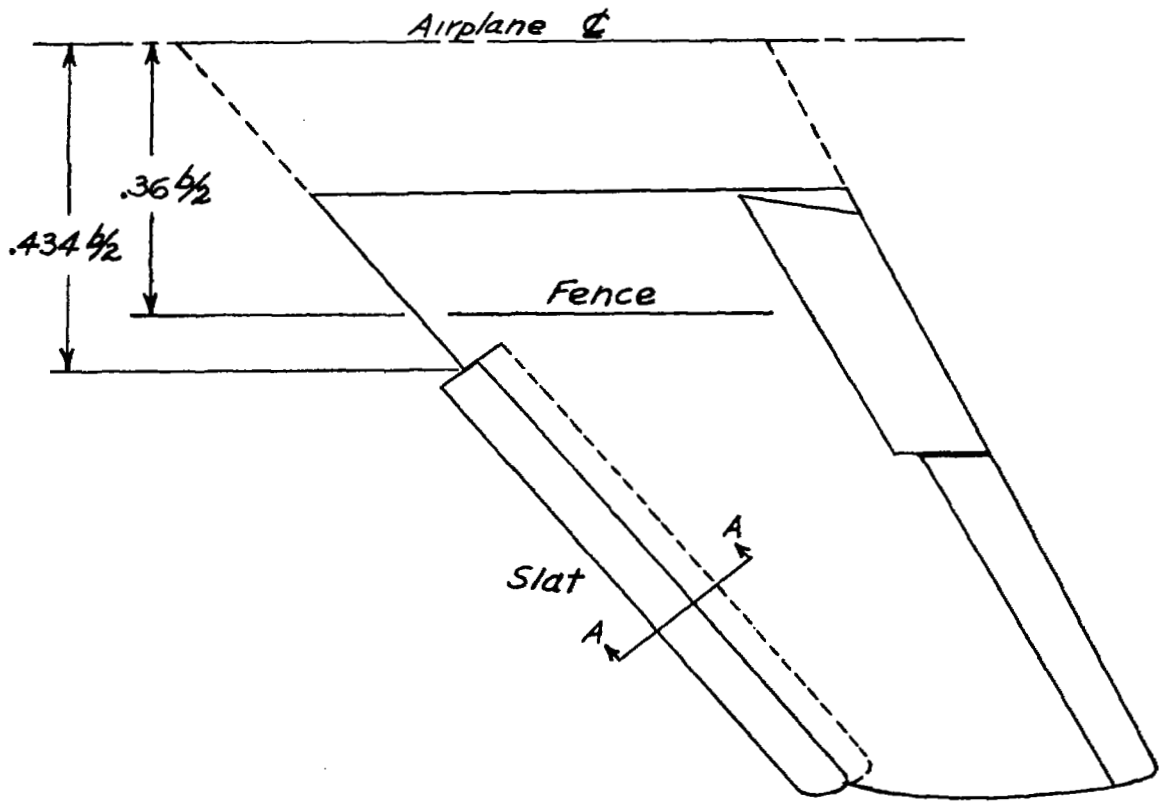

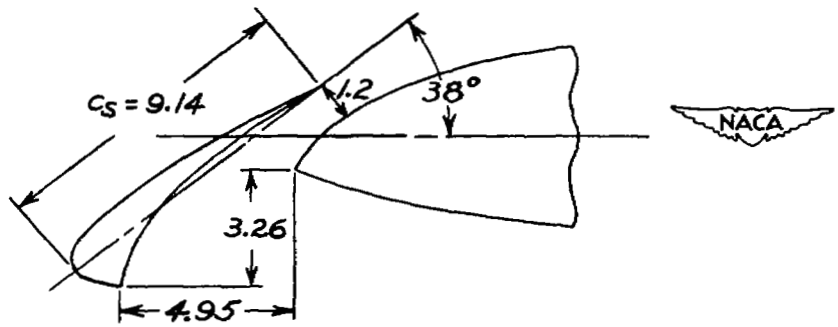

Section A-A (enlarged)

Figure 4.- Sketch of wing and slat. Dimensions given in inches unless otherwise noted.

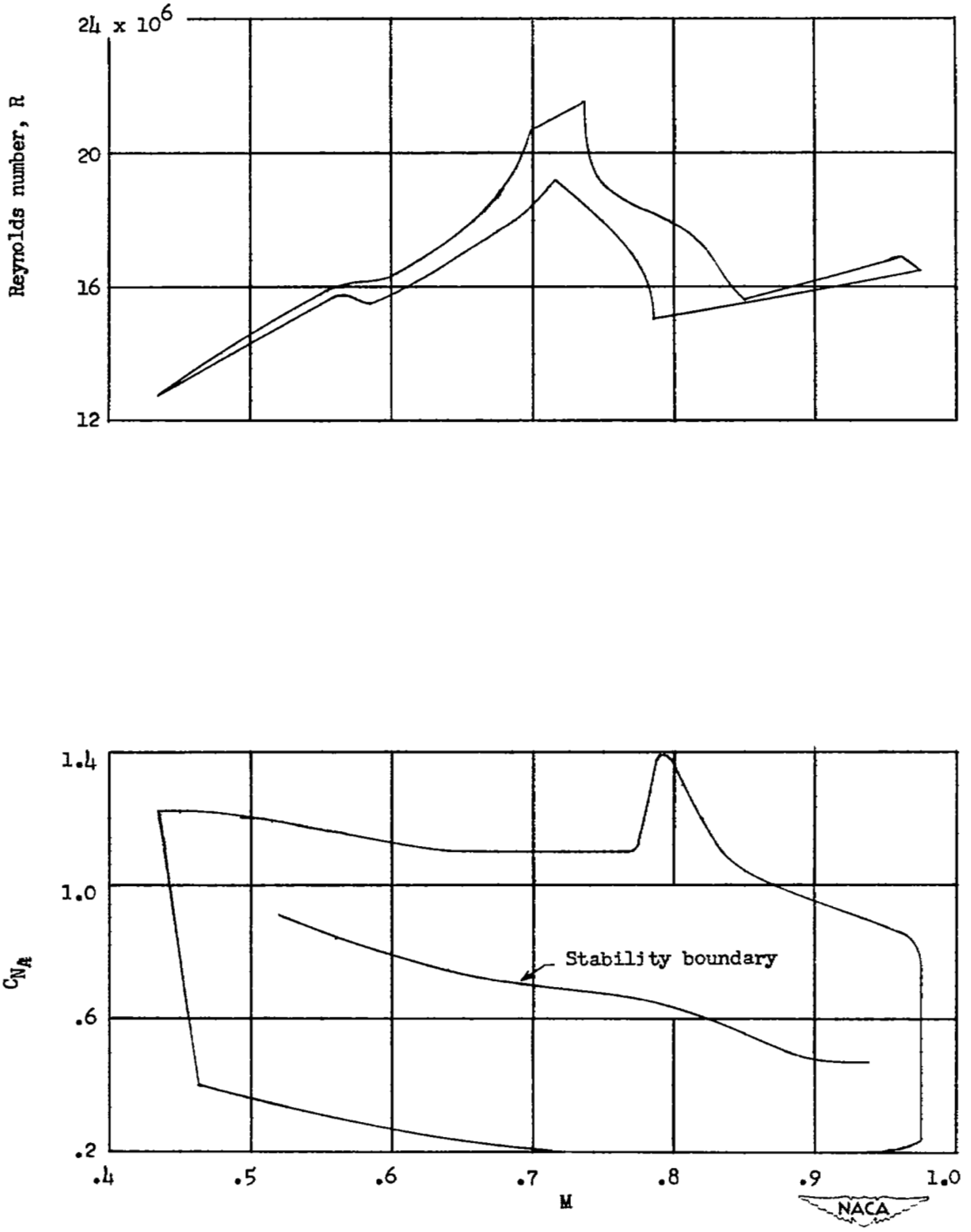

Figure 5.- Reynolds number and airplane normal-force coefficient flight envelopes.

[redacted]

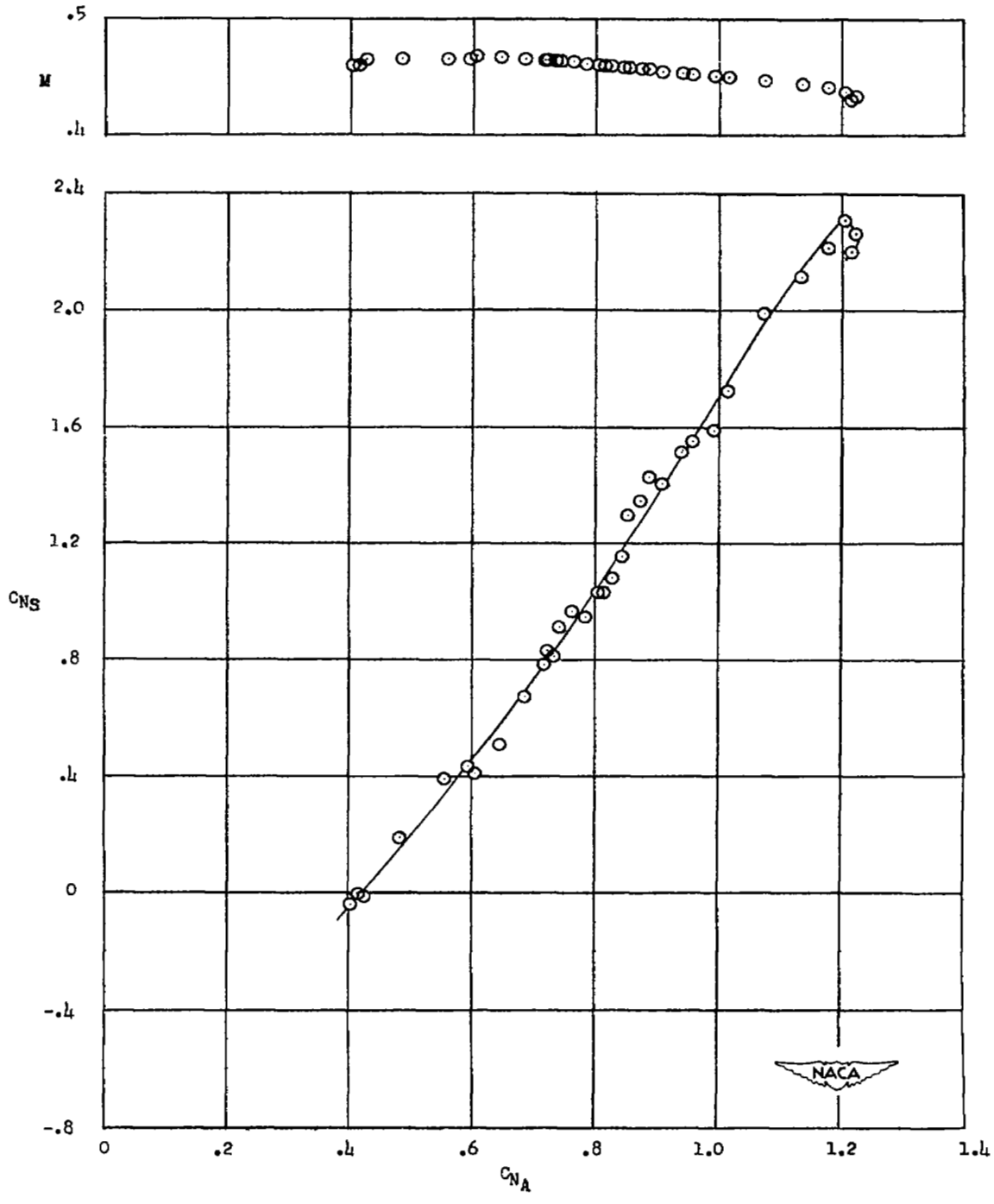

(a) $h_p \approx 19{,}200$ feet.

Figure 6.- Variation of slat normal-force coefficient with airplane normal-force coefficient.

[redacted]

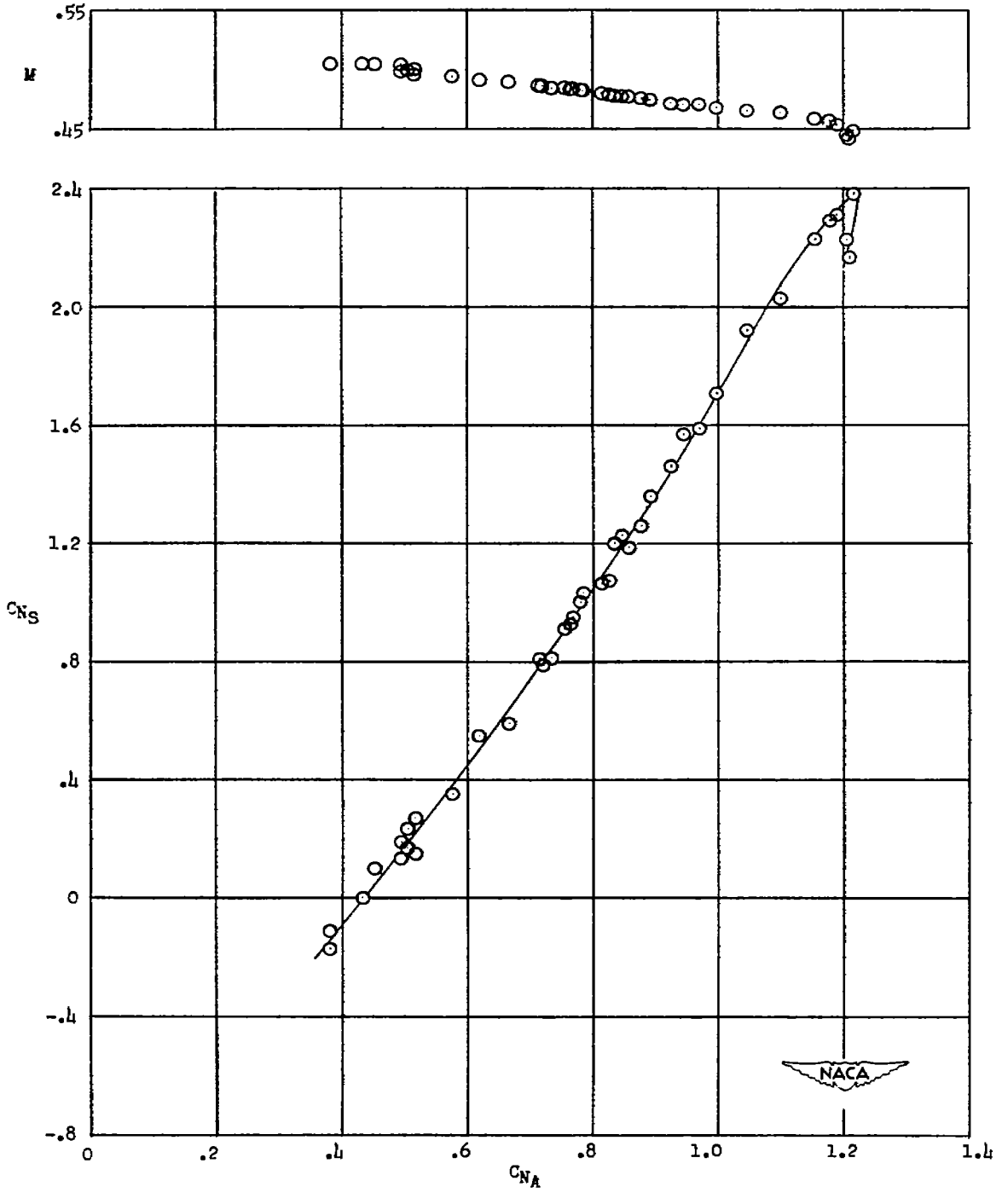

(b) $h_p \approx 19{,}750$ feet.

Figure 6.- Continued.

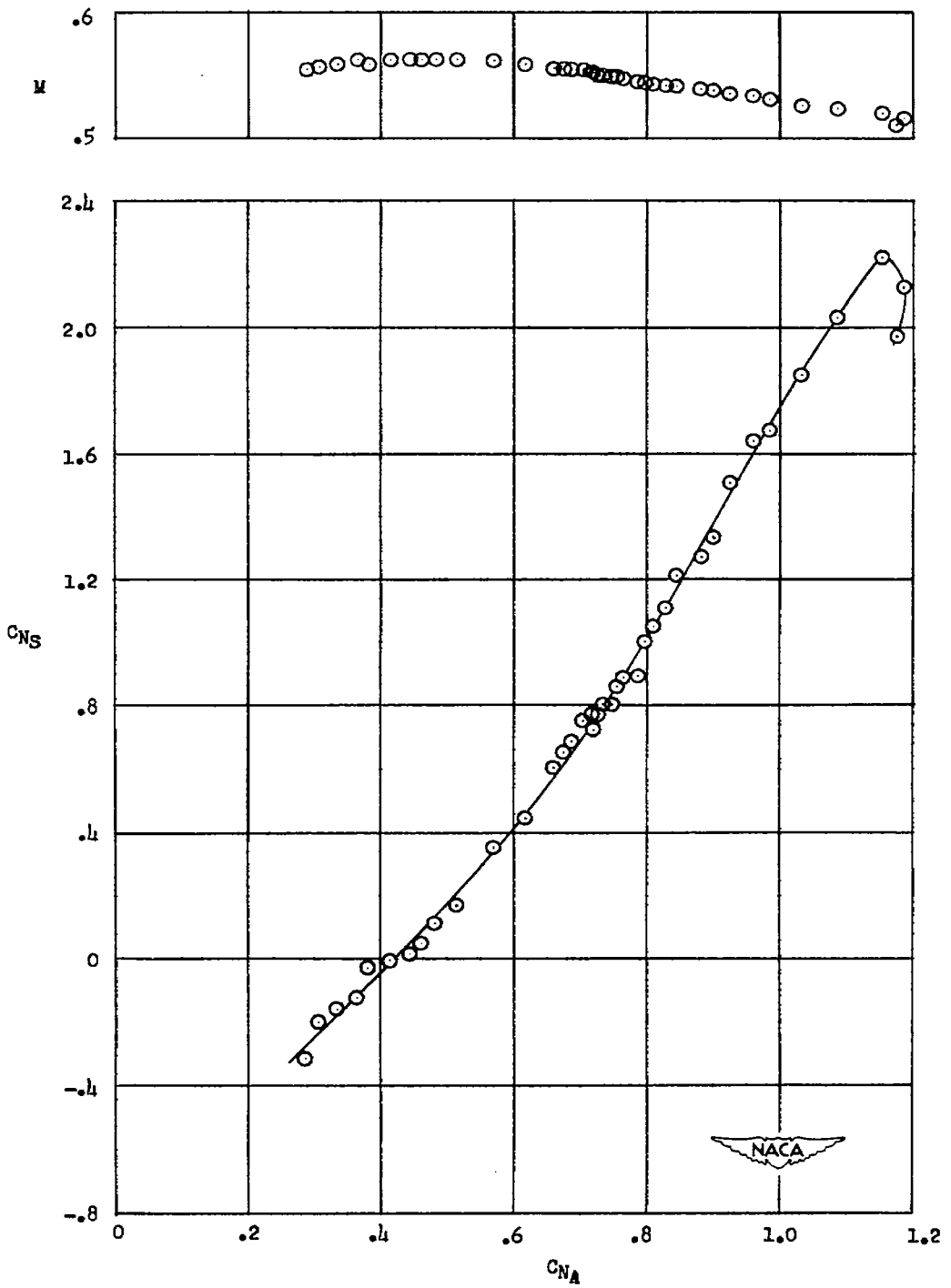

(c) $h_p \approx 19{,}900$ feet.

Figure 6.- Continued.

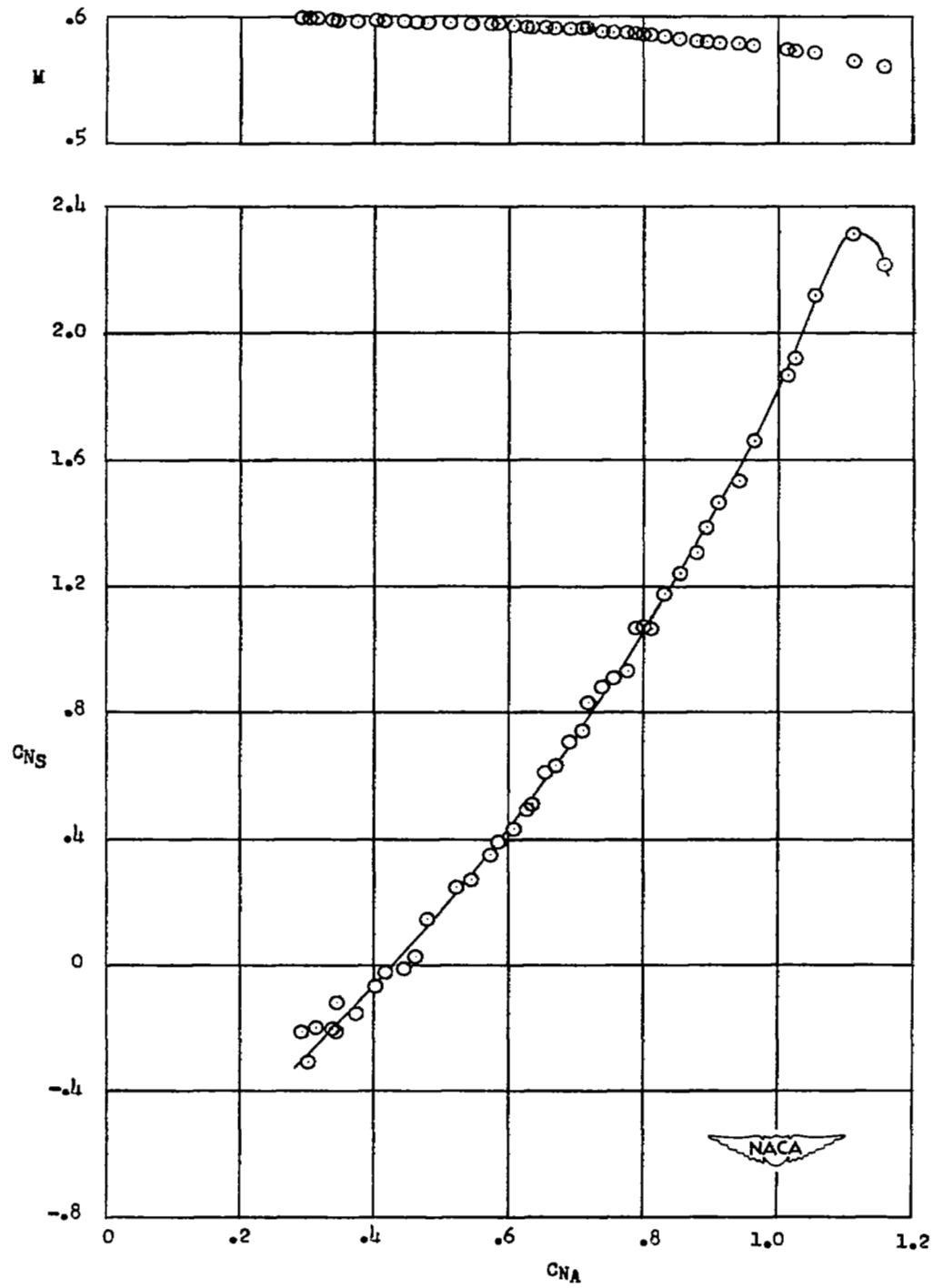

(d) $h_p \approx 21{,}100$ feet.

Figure 6.- Continued.

[redacted]

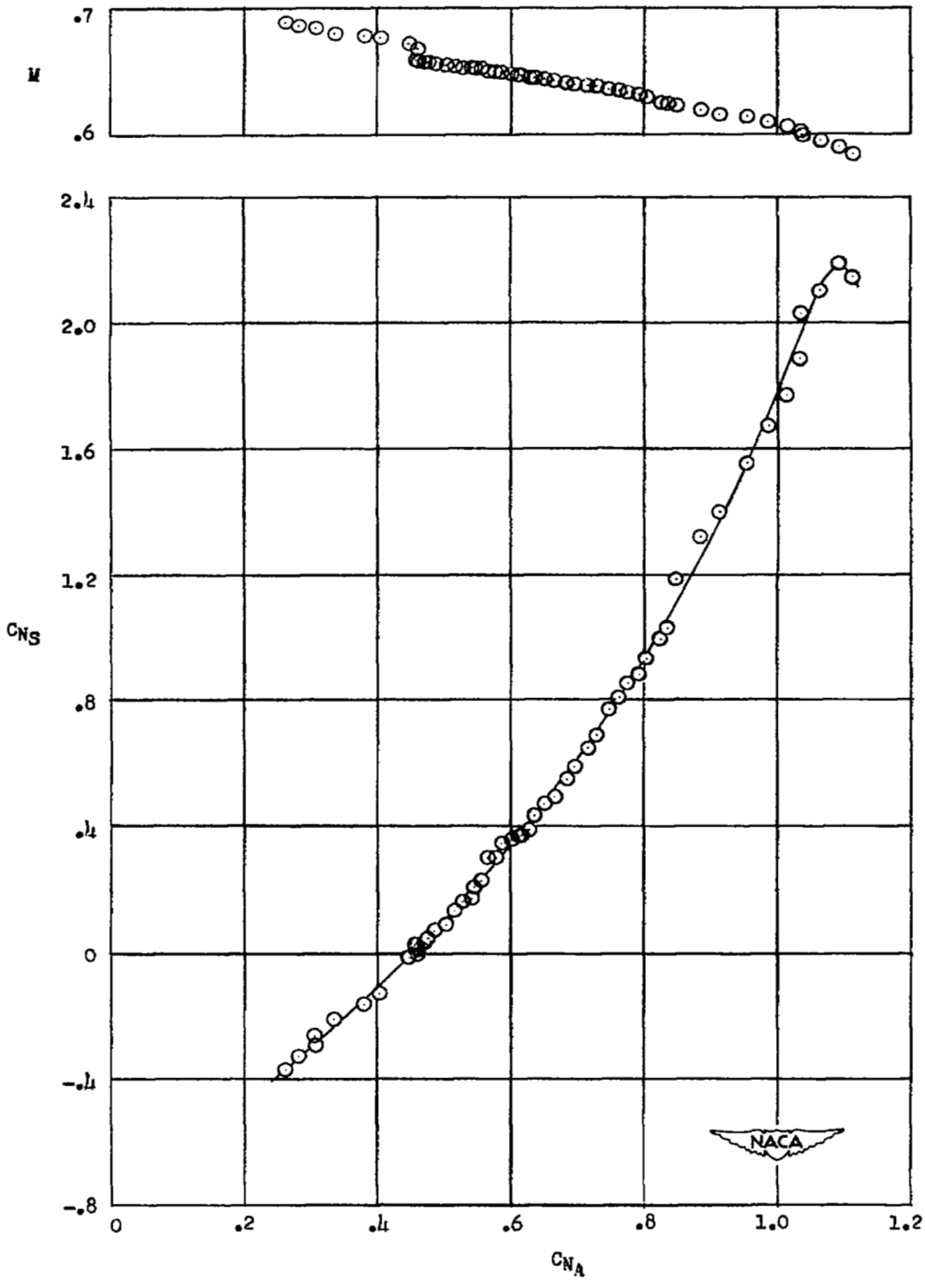

(e) $h_p \approx 22{,}900$ feet.

Figure 6.- Continued.

[redacted]

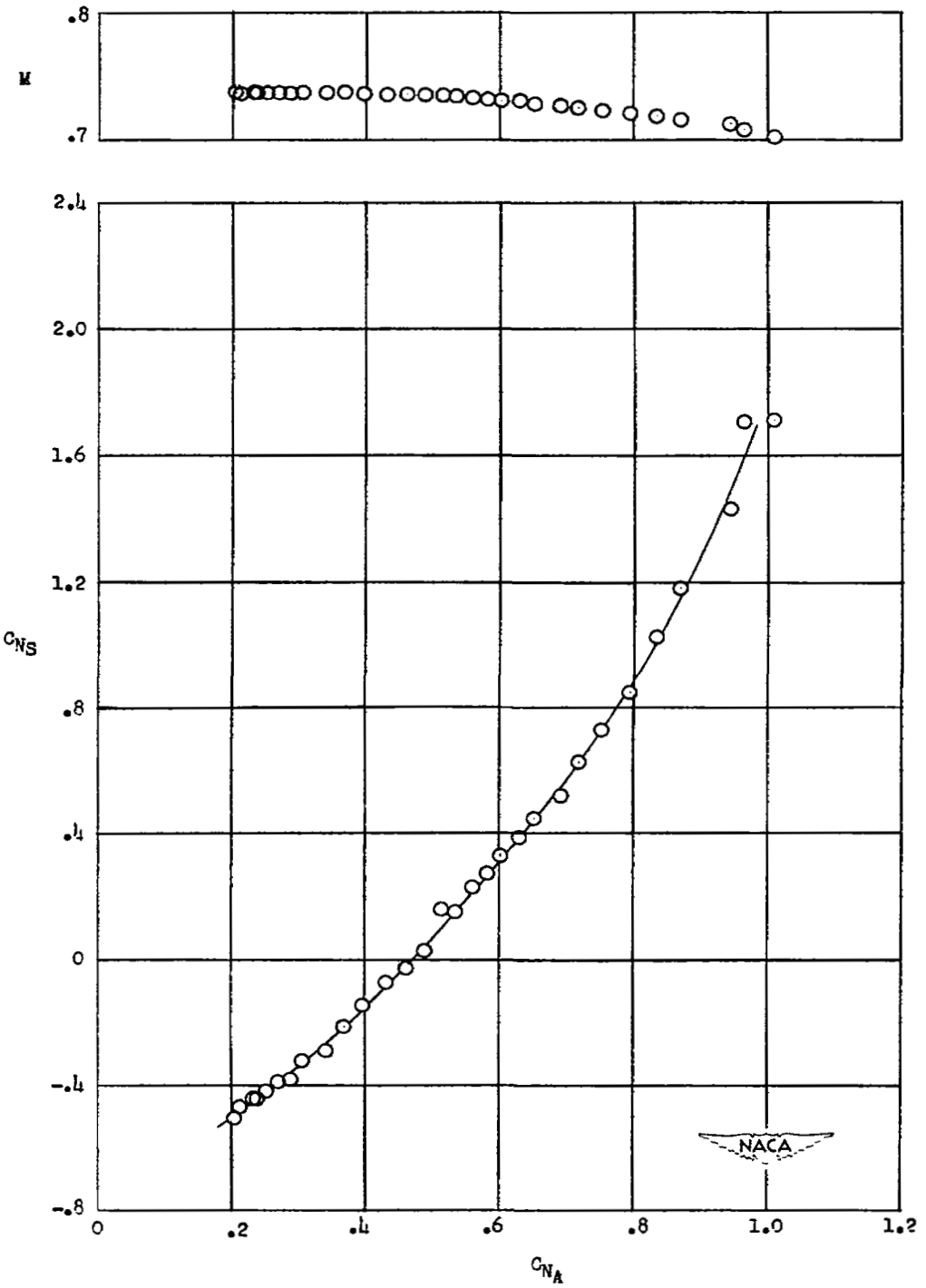

(f) $h_p \approx 19{,}700$ feet.

Figure 6.- Continued.

[redacted]

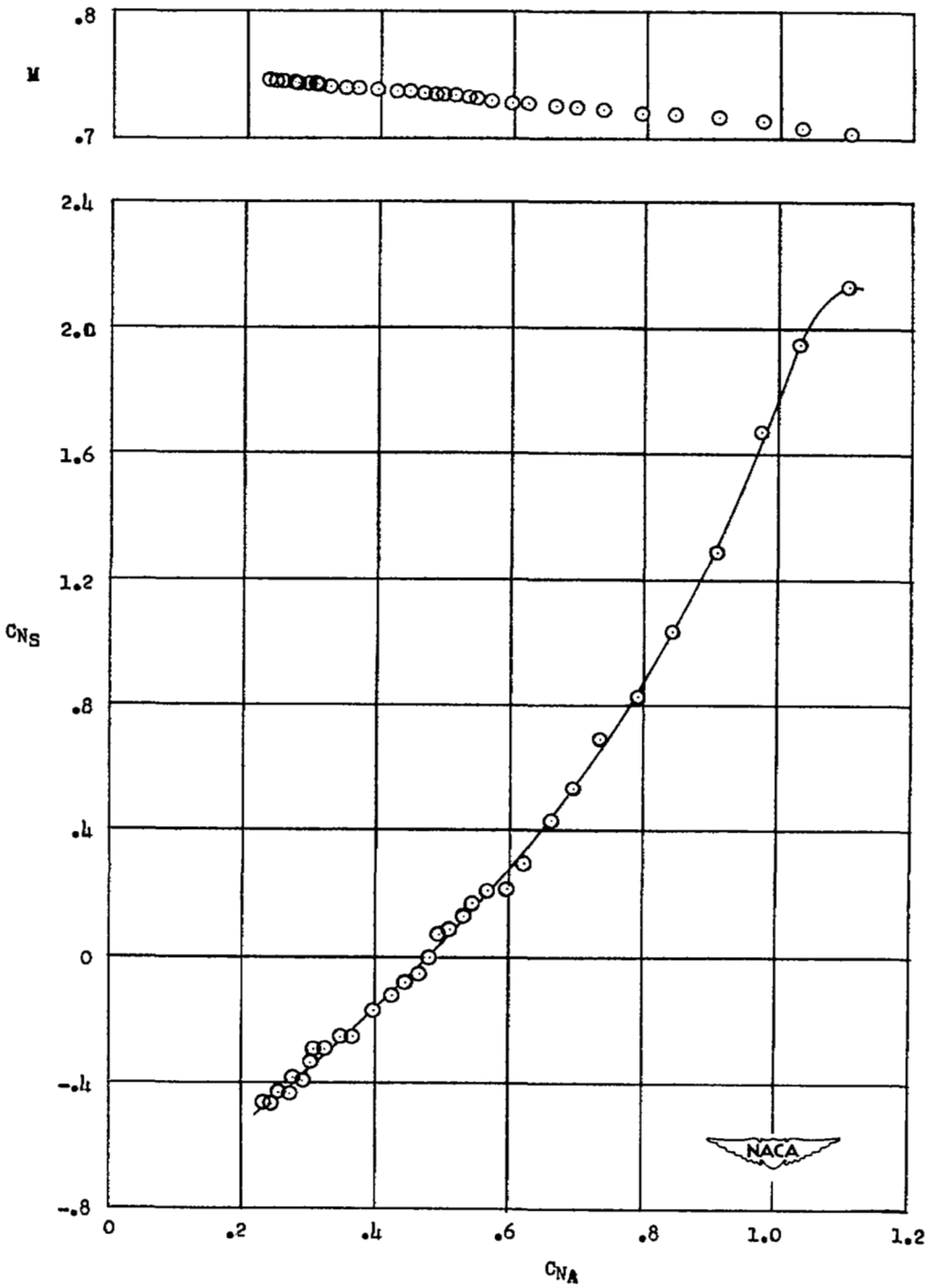

(g) $h_p \approx 23,900$ feet.

Figure 6.- Continued.

[redacted]

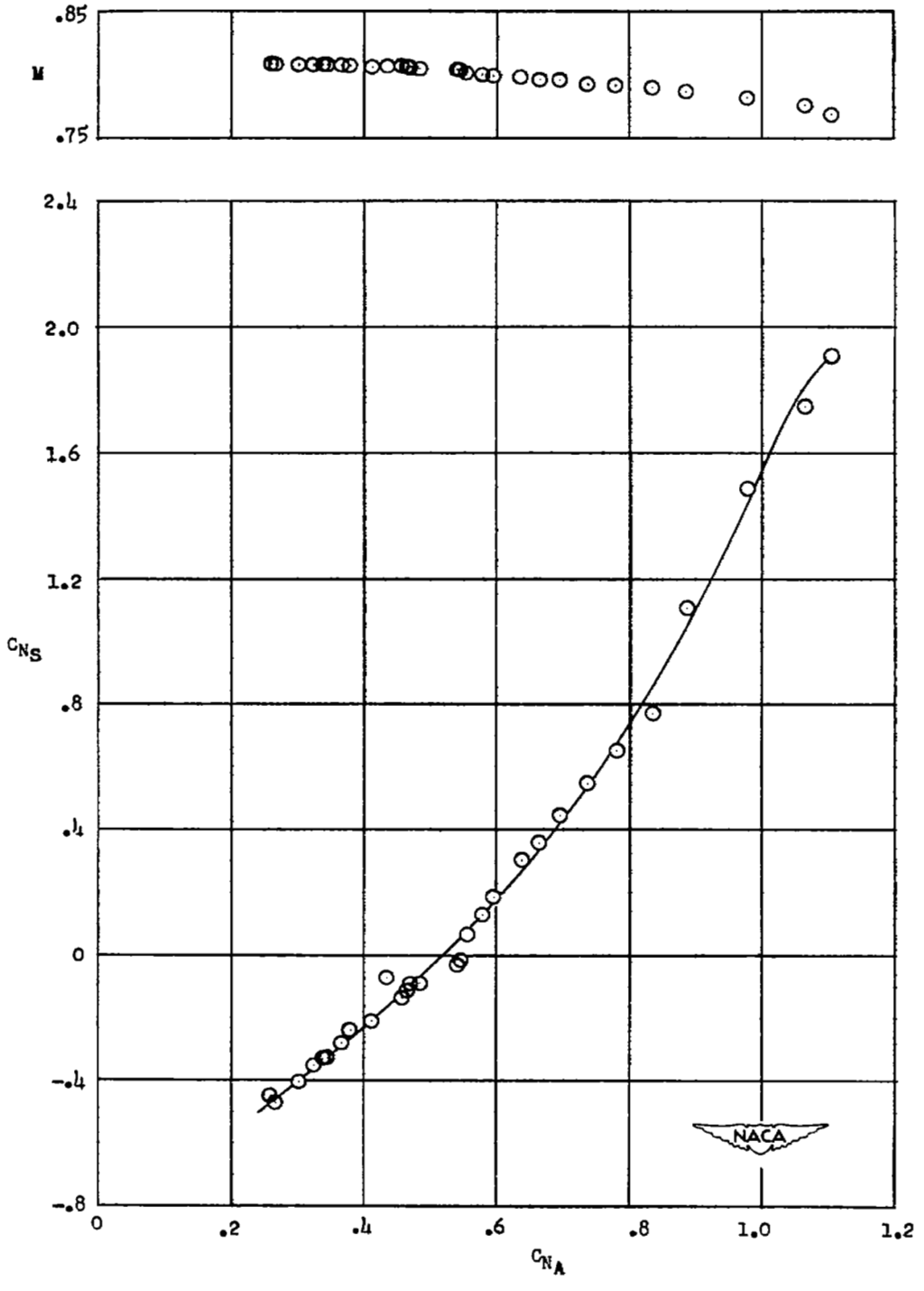

(h) $h_p \approx 28{,}600$ feet.

Figure 6.- Continued.

[redacted]

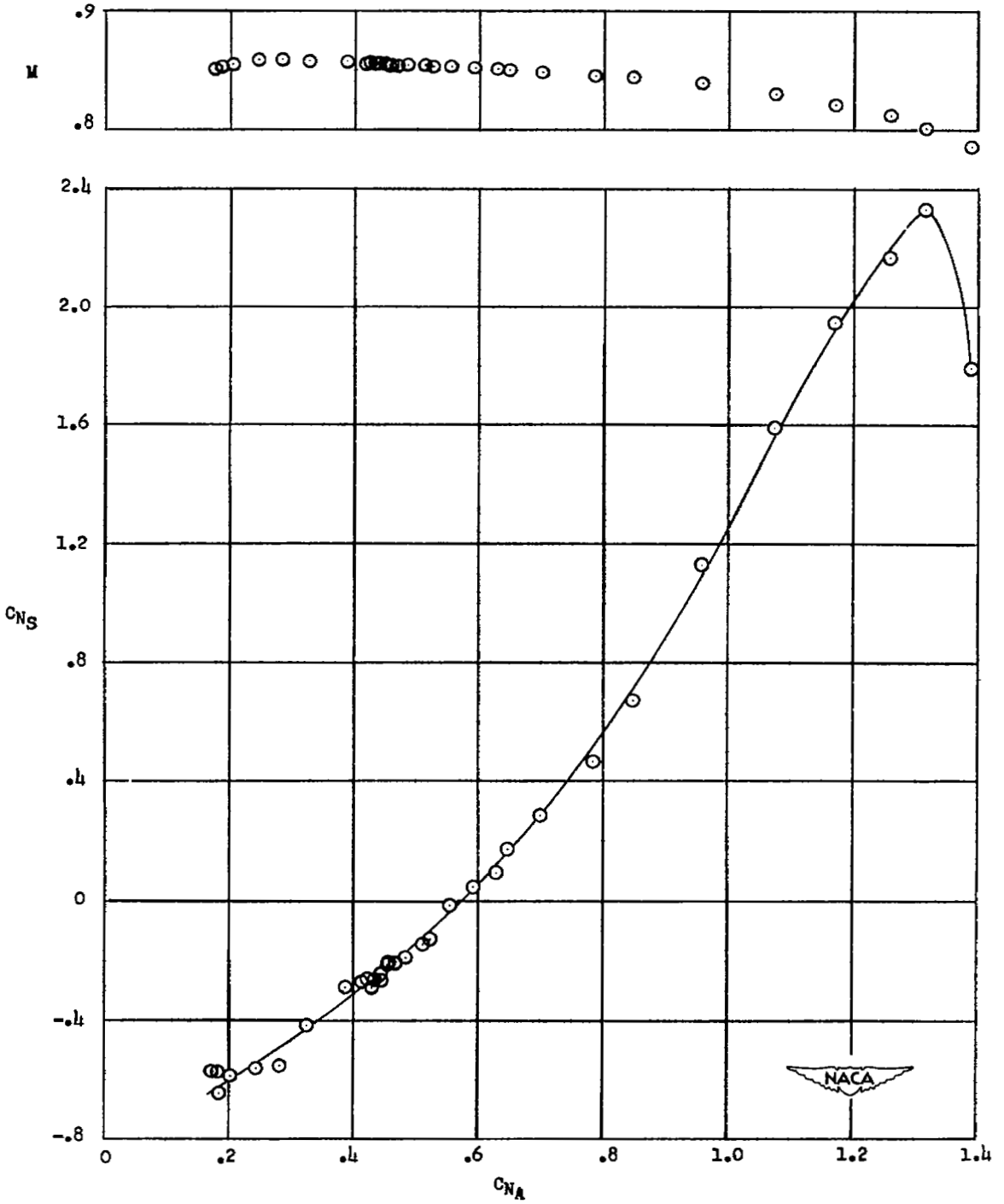

(i) $h_p \approx 32{,}900$ feet.

Figure 6.- Continued.

[redacted]

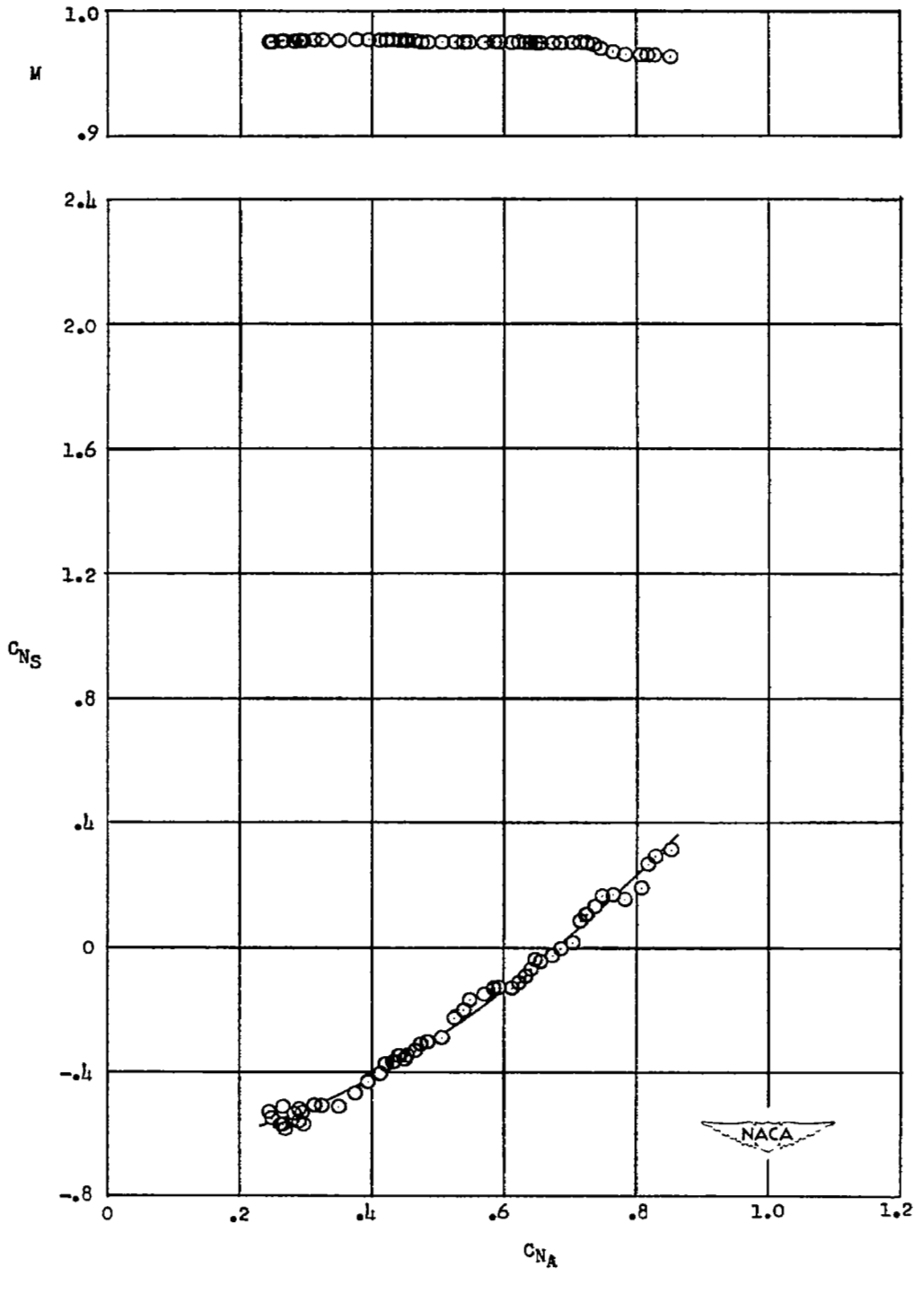

(j) $h_p \approx 34,200$ feet.

Figure 6.- Concluded.

[redacted]

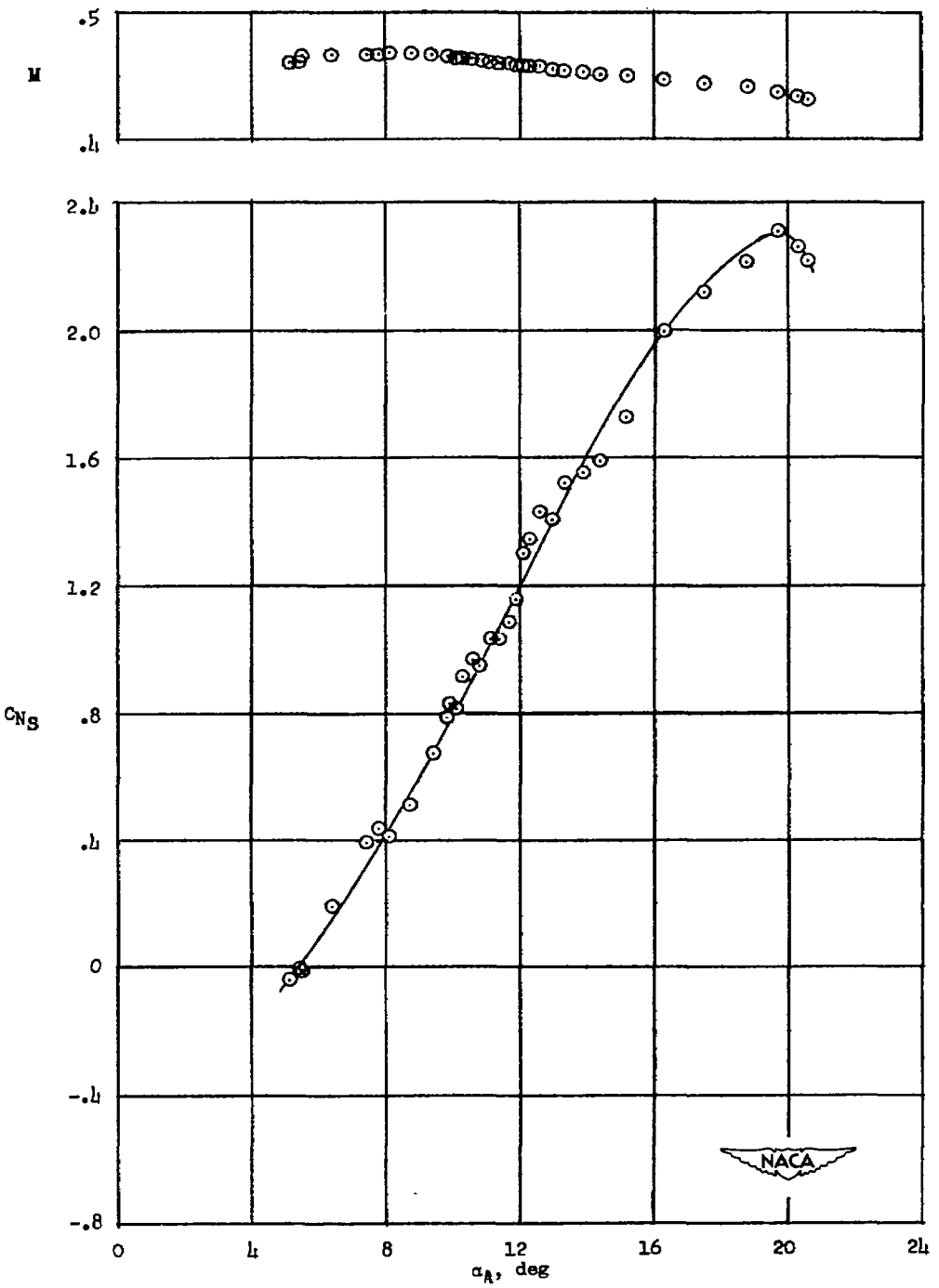

(a) $h_p \approx 19{,}200$ feet.

Figure 7.- Variation of slat normal-force coefficient with airplane angle of attack.

[redacted]

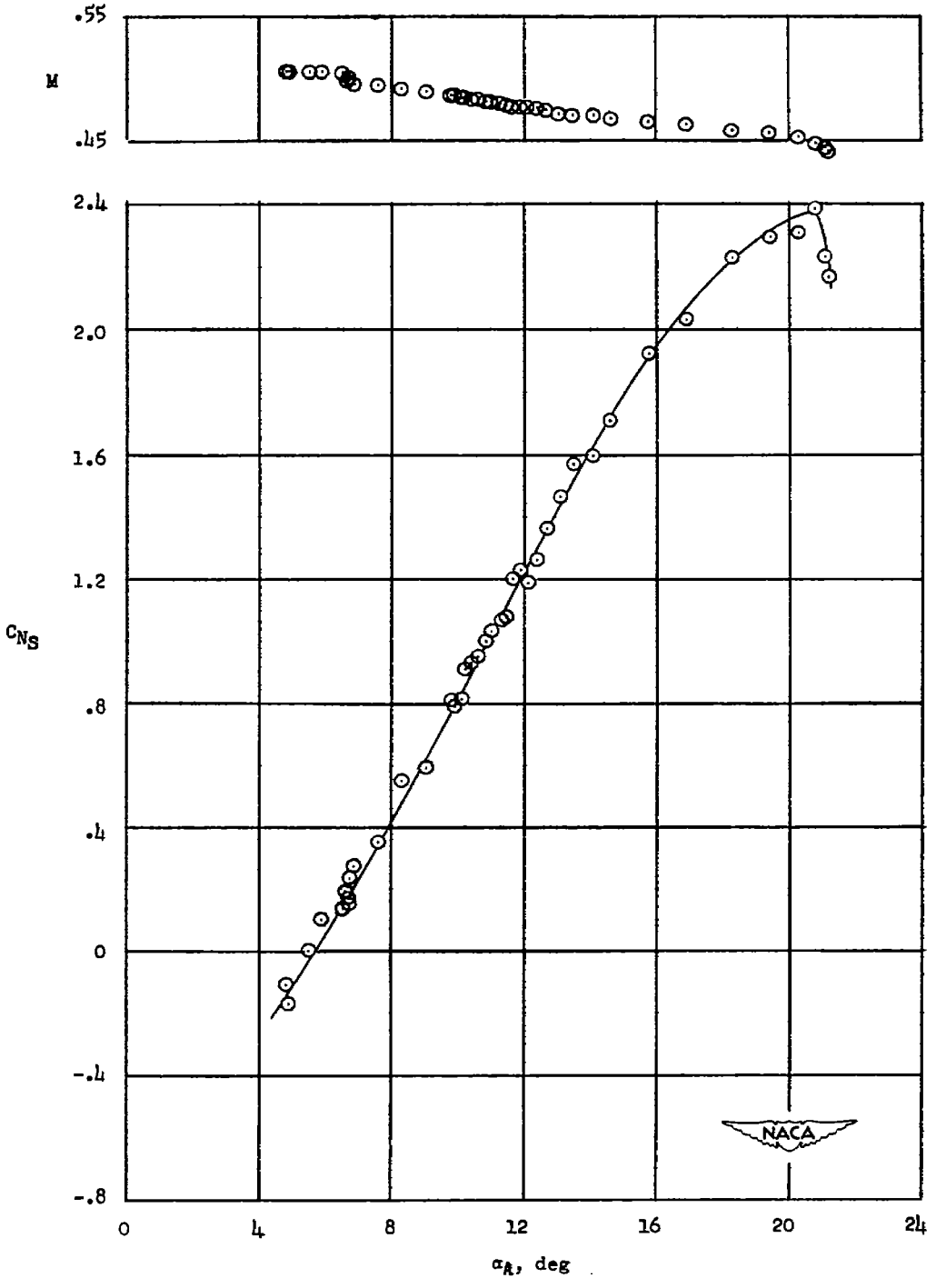

(b) $h_p \approx 19{,}750$ feet.

Figure 7.- Continued.

[redacted]

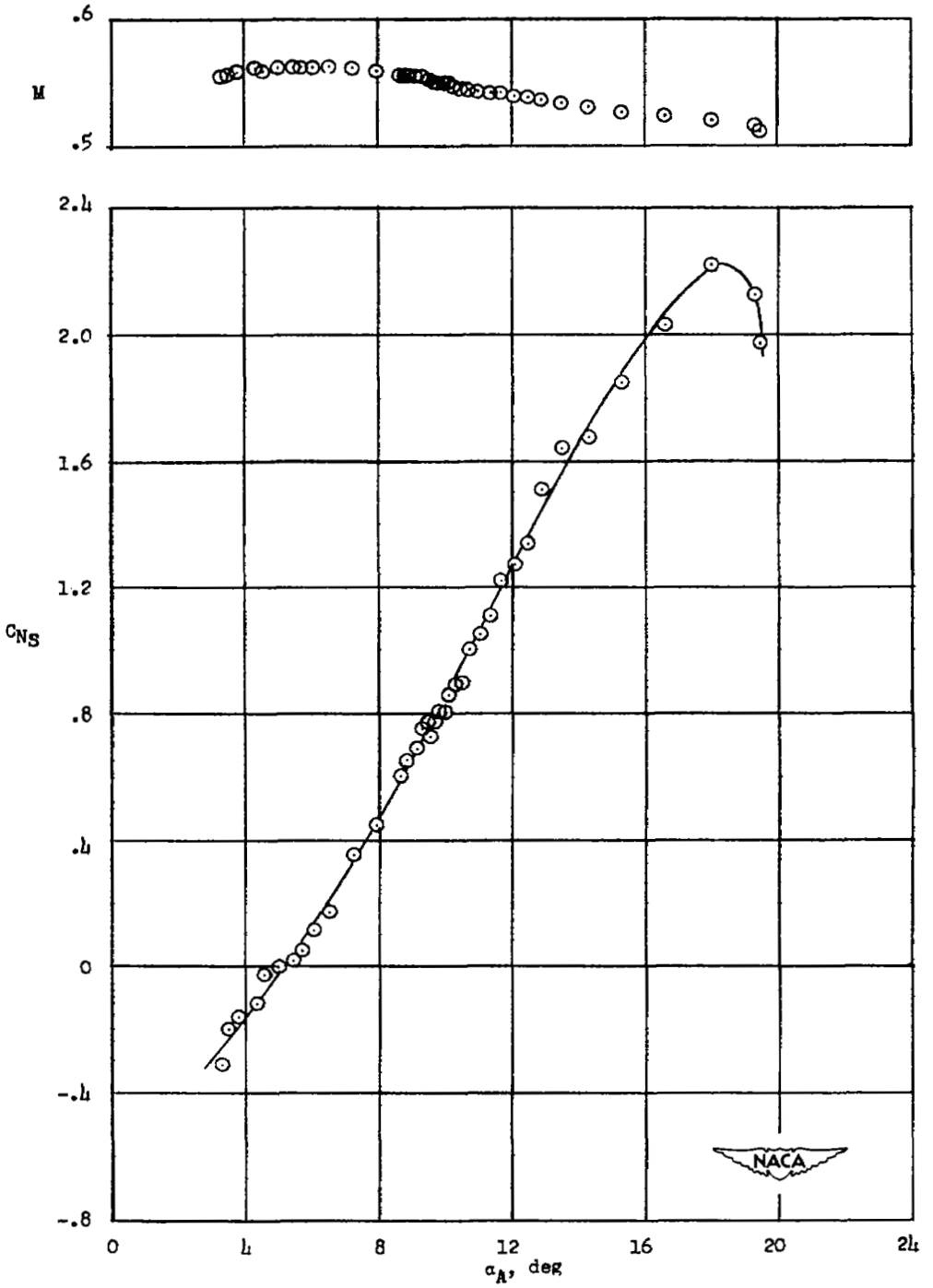

(c) $h_p \approx 19{,}900$ feet.

Figure 7.- Continued.

[redacted]

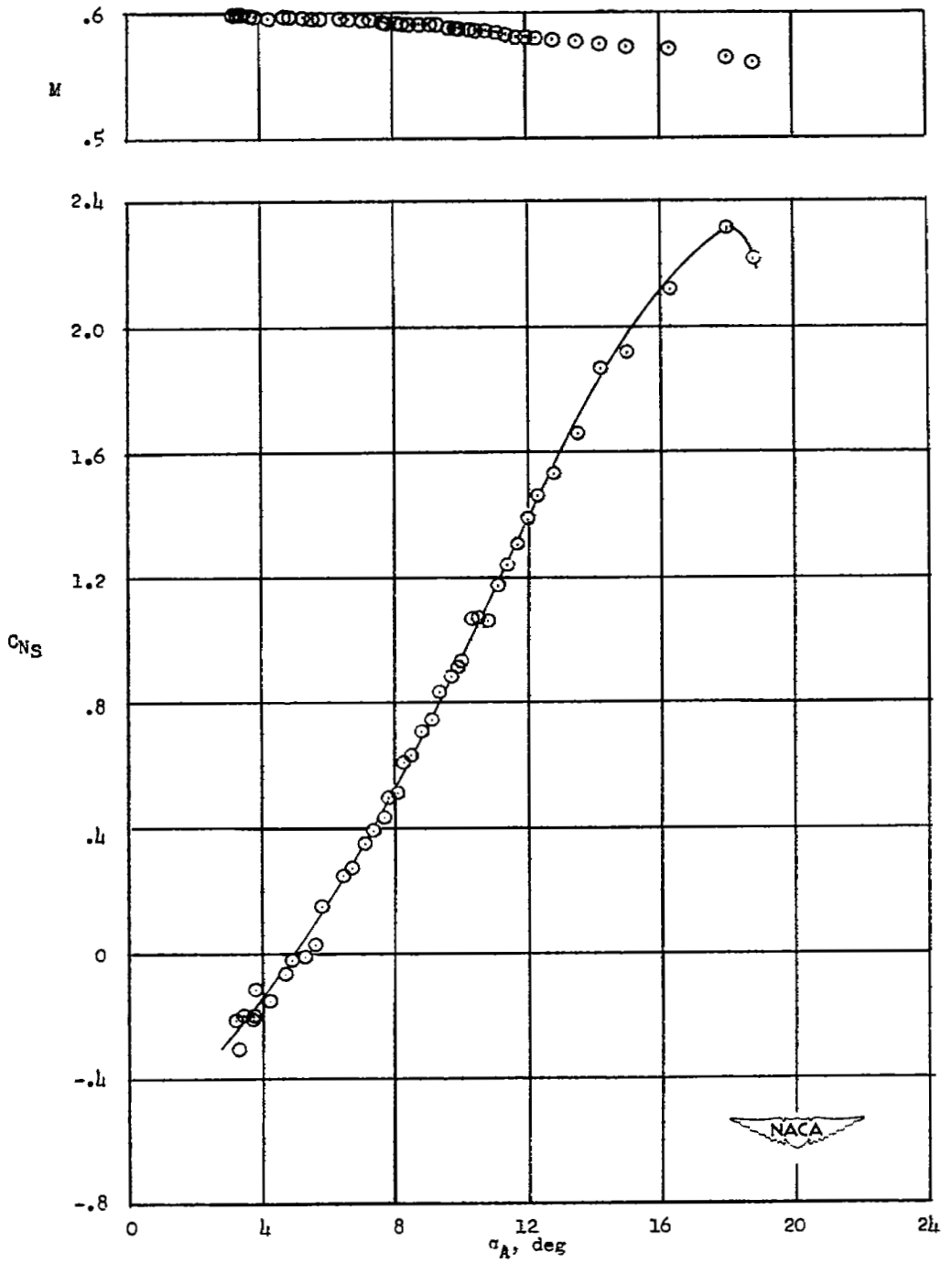

(d) $h_p \approx 21{,}100$ feet.

Figure 7.- Continued.

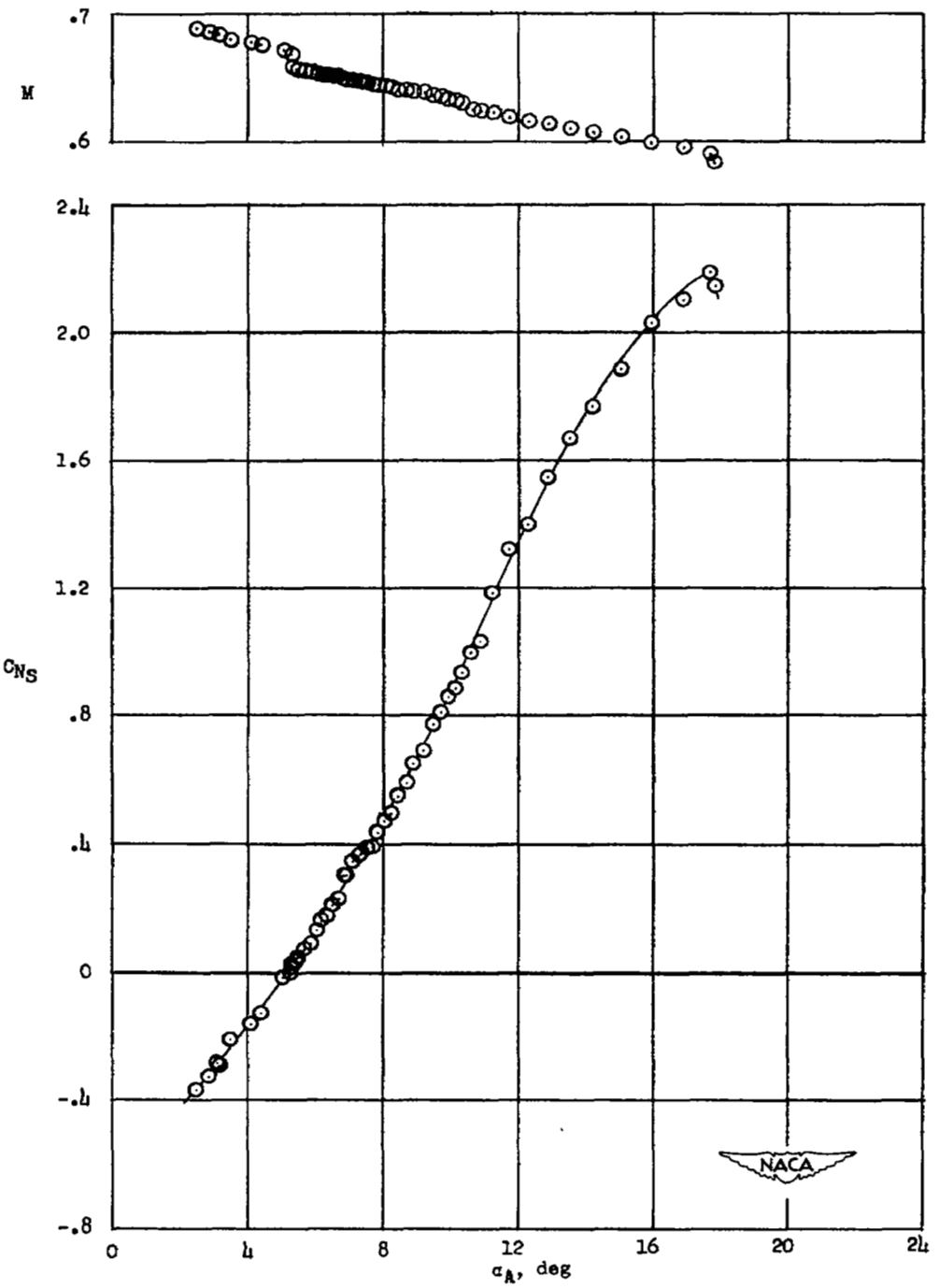

(e) $h_p \approx 22{,}900$ feet.

Figure 7.- Continued.

[redacted]

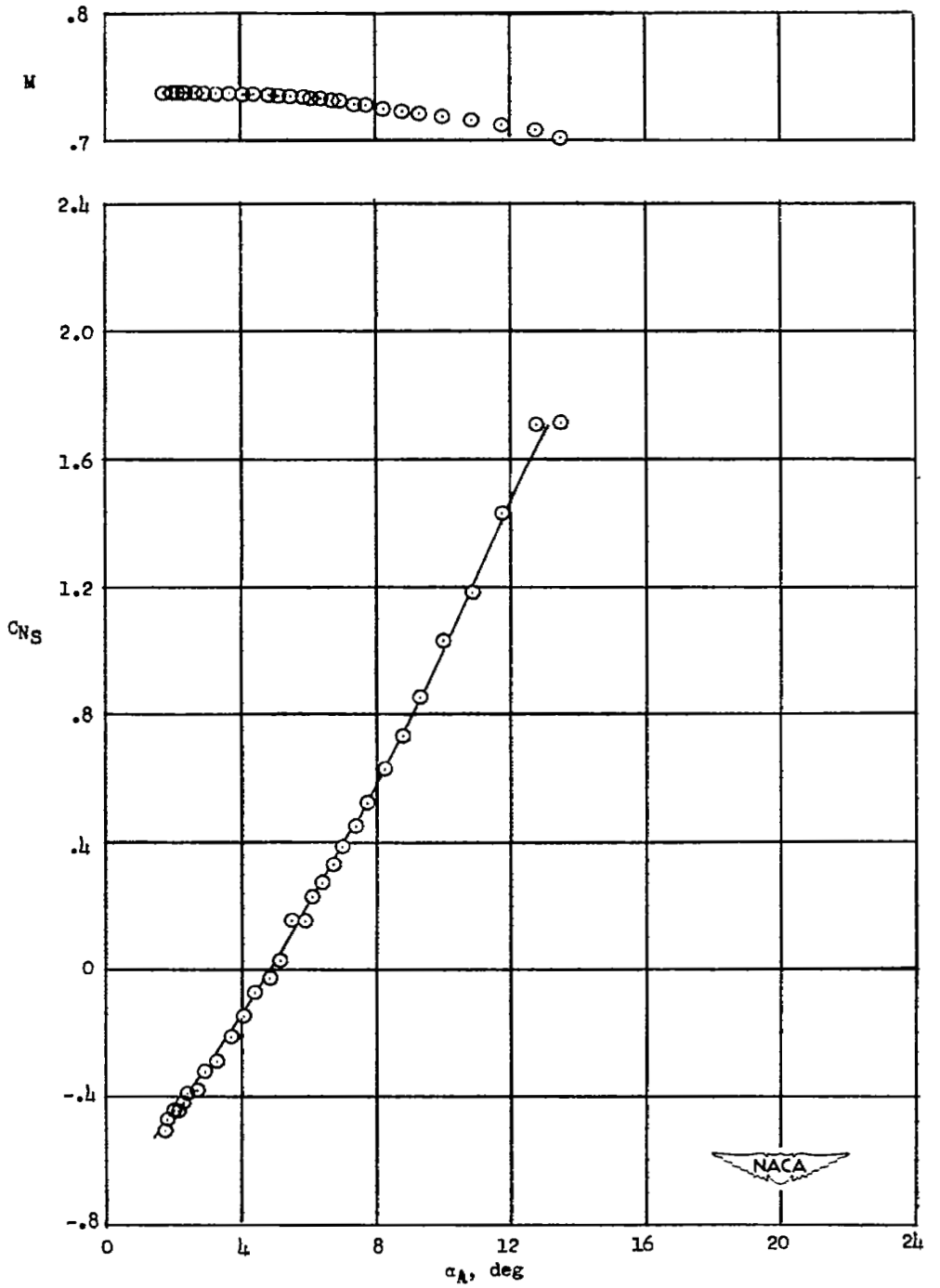

(f) $h_p \approx 19{,}700$ feet.

Figure 7.- Continued.

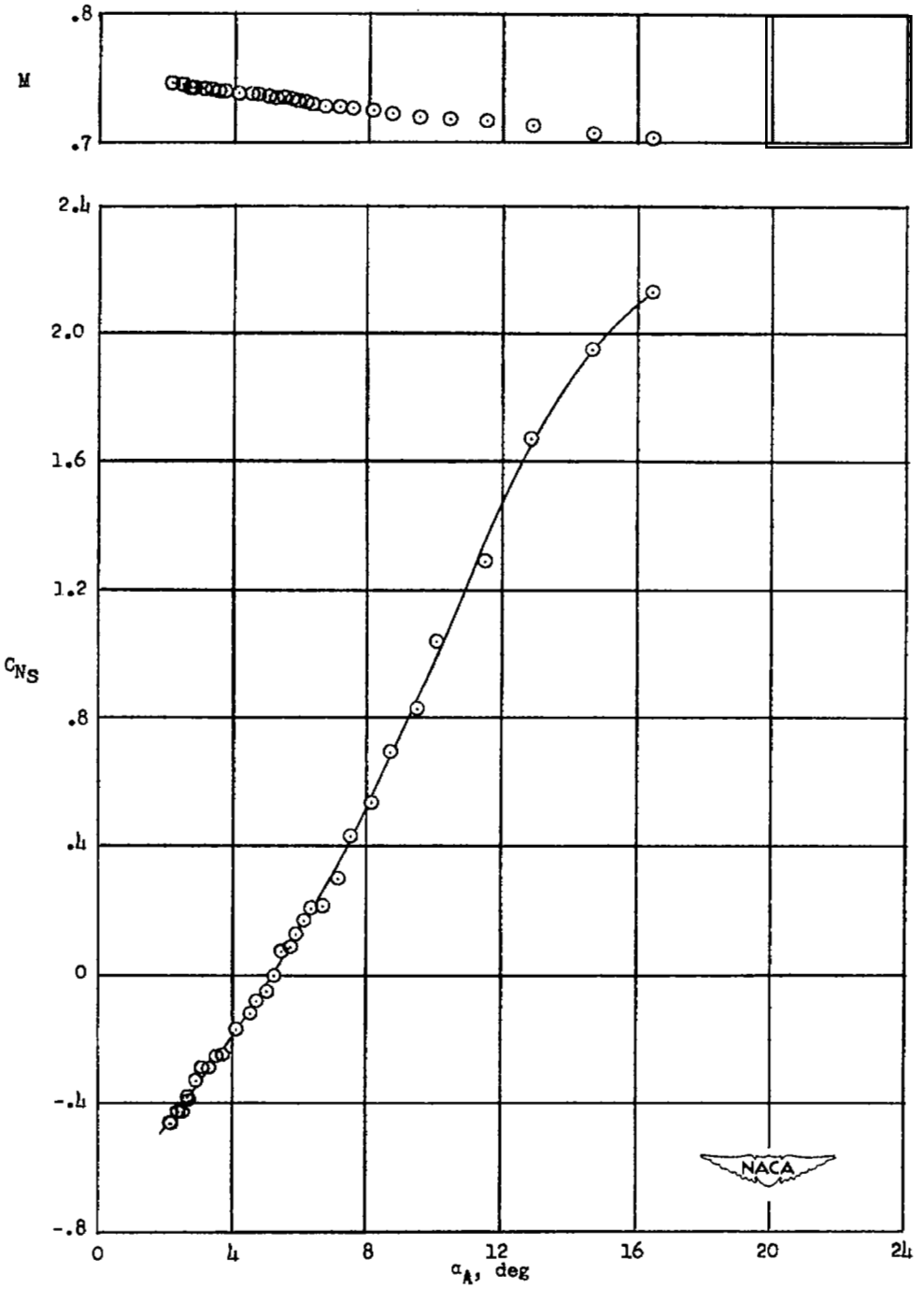

(g) $h_p \approx 23{,}900$ feet.

Figure 7.- Continued.

[redacted]

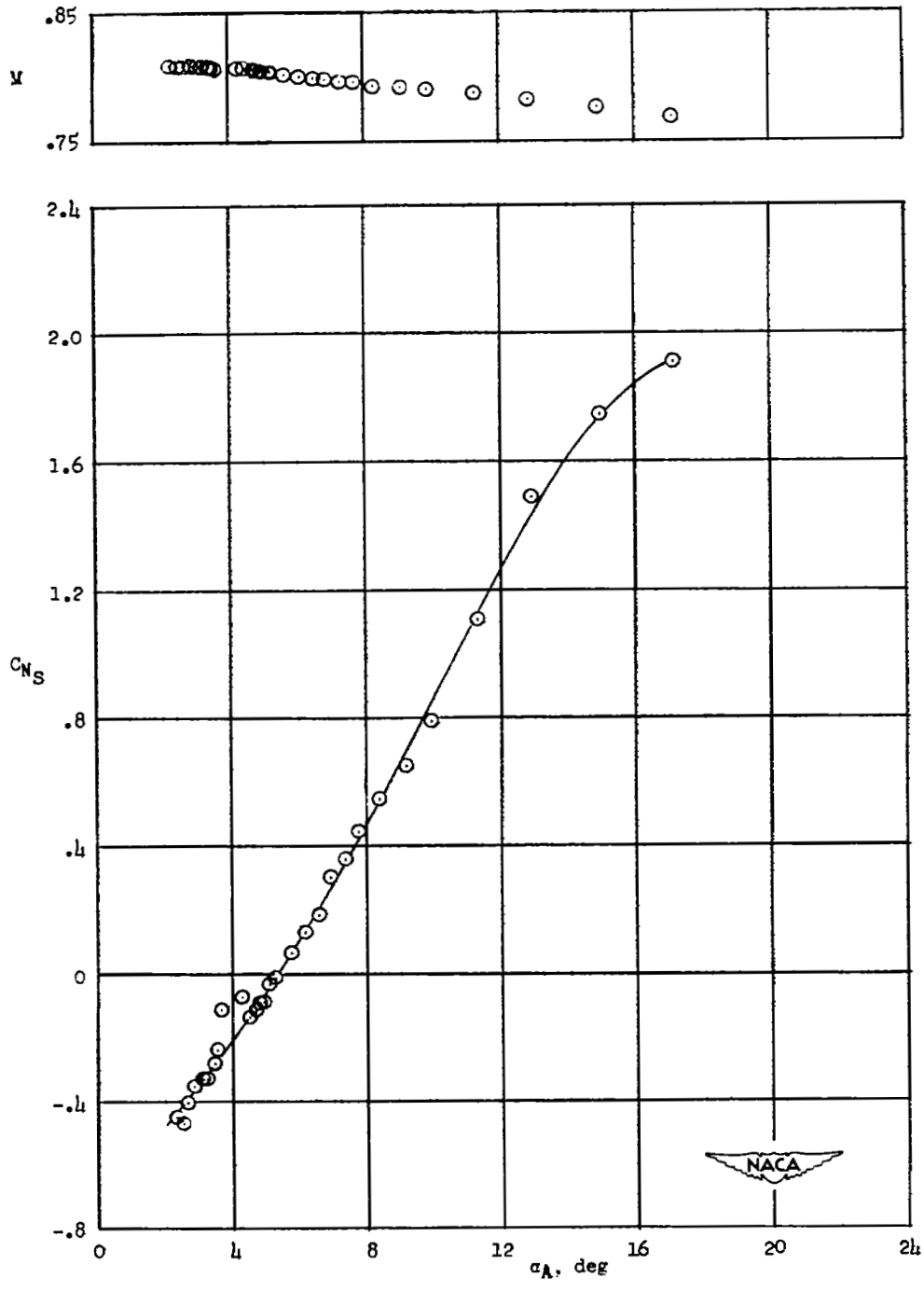

(h) $h_p \approx 28{,}600$ feet.

Figure 7.- Continued.

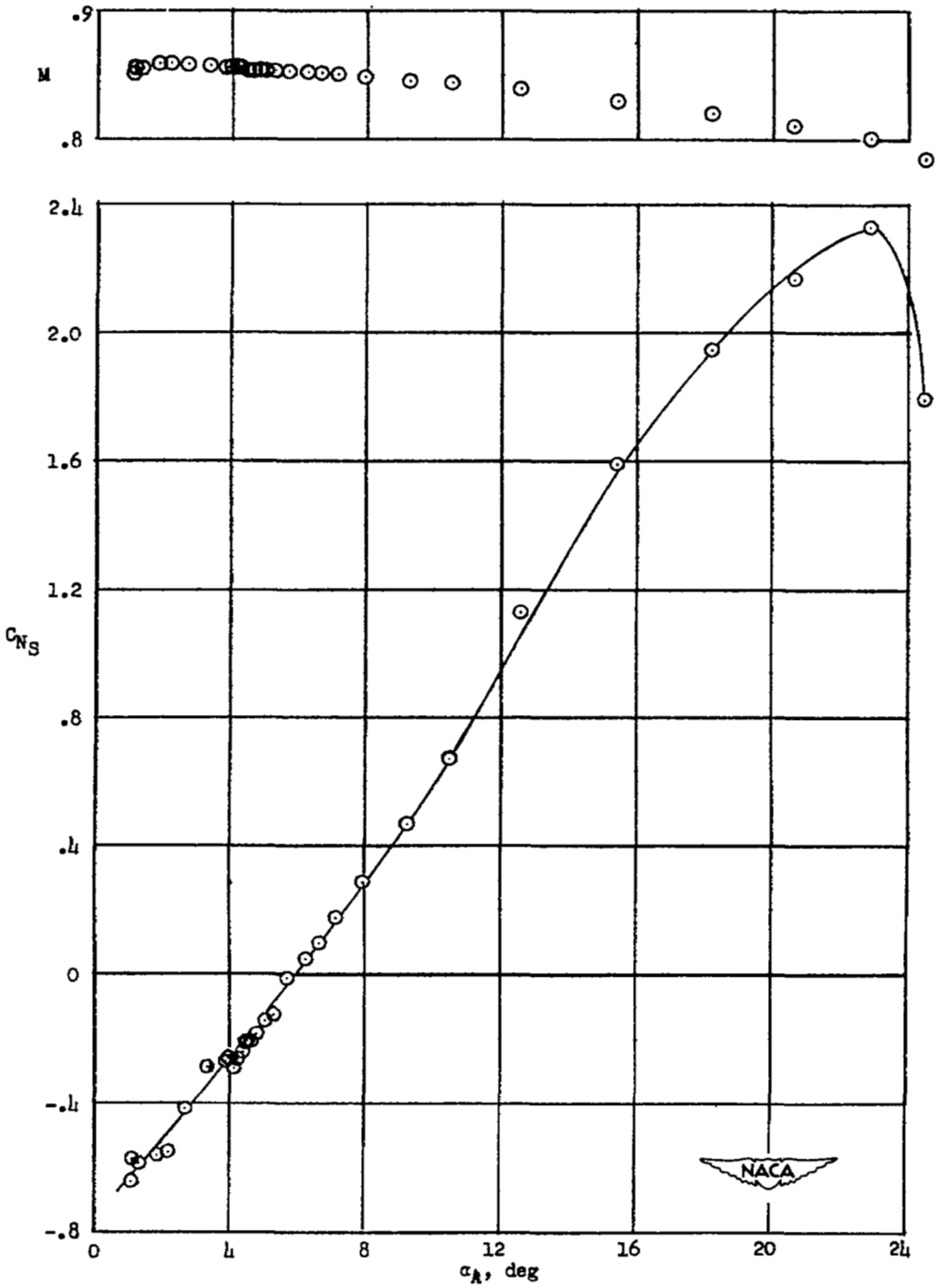

(i) $h_p \approx 32{,}900$ feet.

Figure 7.- Continued.

[redacted]

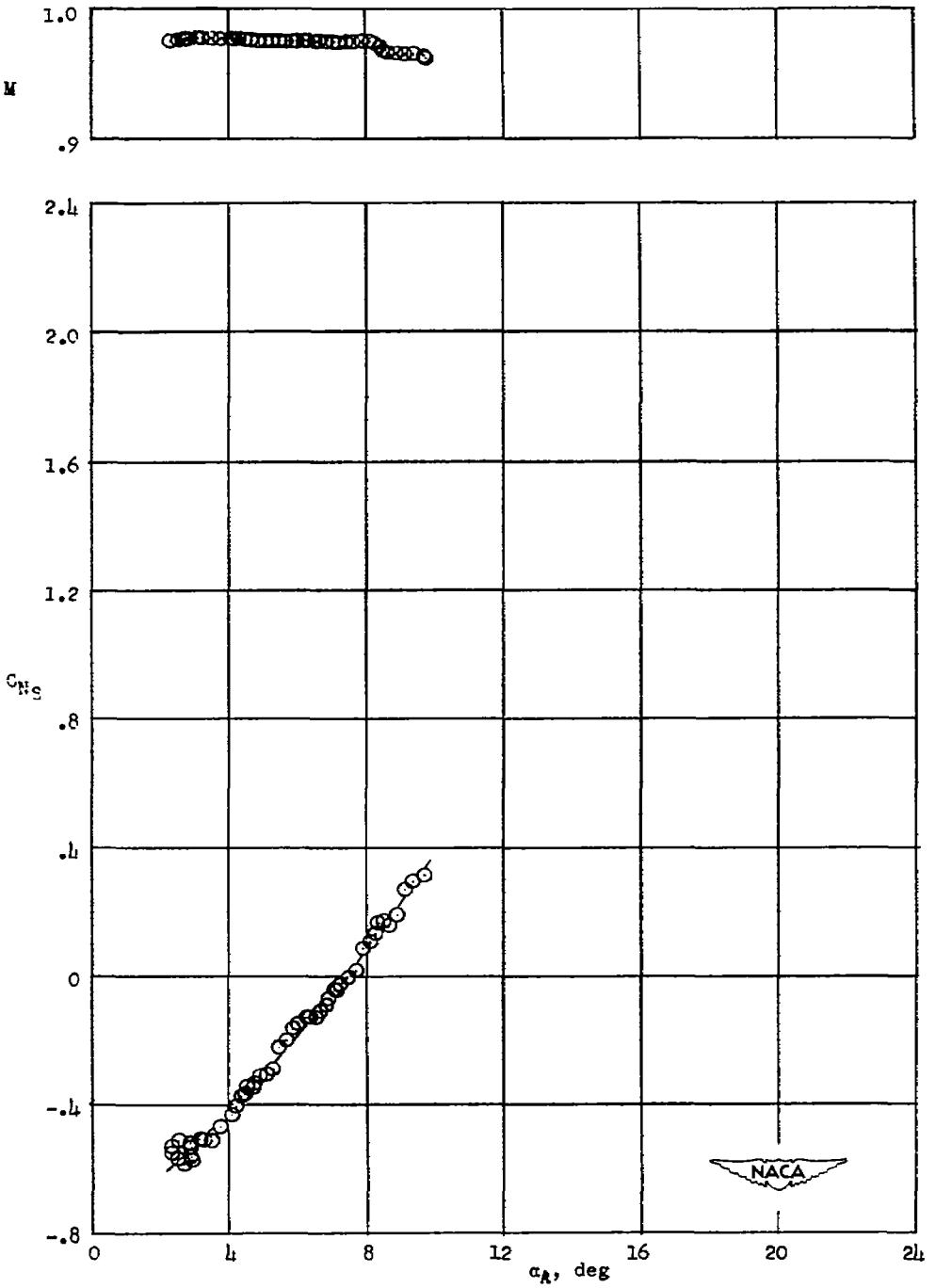

(j) $h_p \approx 34{,}200$ feet.

Figure 7.- Concluded.

[redacted]

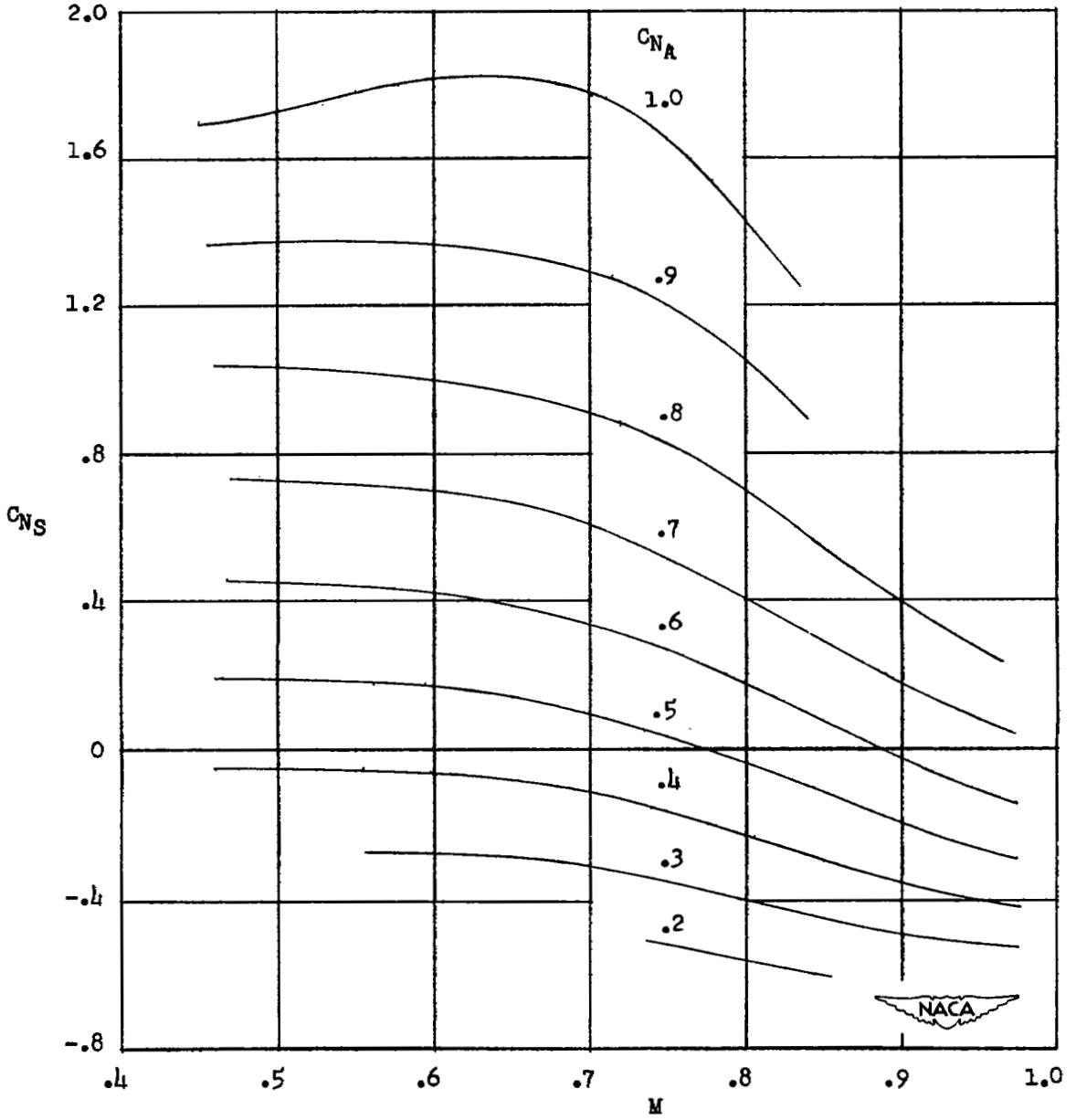

Figure 8.- Variation of slat normal-force coefficient with Mach number for constant values of airplane normal-force coefficient.

[redacted]

NACA-Langley - 8-27-53 - 325

[redacted]

[redacted]